



THESIS

1

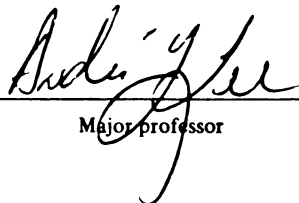
This is to certify that the
thesis entitled
EFFECT OF CROSSLINK DENSITY DISTRIBUTION ON MECHANICAL
RESPONSES OF PHYSICALLY AGED EPOXY GLASSES

presented by

Yitong Wang

has been accepted towards fulfillment
of the requirements for

Master's degree in Materials Science


Major professor

Date June 16, 1995

**LIBRARY
Michigan State
University**

**PLACE IN RETURN BOX to remove this checkout from your record.
TO AVOID FINES return on or before date due.**

DATE DUE	DATE DUE	DATE DUE
_____	_____	_____
_____	_____	_____
_____	_____	_____
_____	_____	_____
_____	_____	_____
_____	_____	_____
_____	_____	_____

MSU is An Affirmative Action/Equal Opportunity Institution

c:\crl\data\due.pm3-p.1

**EFFECT OF CROSSLINK DENSITY DISTRIBUTION ON MECHANICAL
RESPONSES OF PHYSICALLY AGED EPOXY GLASSES**

By

Yitong Wang

A THESIS

**Submitted to
Michigan State University
in partial fulfillment of the requirements
for the degree of**

MASTER OF SCIENCE

Department of Materials Science and Mechanics

1995

ABSTRACT

EFFECT OF CROSSLINK DENSITY DISTRIBUTION ON MECHANICAL RESPONSES OF PHYSICALLY AGED EPOXY GLASSES

By

Yitong Wang

A series of epoxy resin were crosslinked with diamine of known molecular weight distribution to form network of control crosslink density distribution. The mechanical properties such as, the fracture toughness, K_{IC} , creep compliance under small step stresses, $D(t)$, and small strain stress relaxation, $E(t)$, of these networks were investigated as function of time and temperature. In fracture experiment, it was found that one was able to increase the K_{IC} with increases in molecular weight of diamine used. Interestingly, the fracture toughness also increase with longer aging time for network containing high fraction of longer molecular weight diamine. This is in contrast with observation of aging effect on single component of polymeric glasses which the value of K_{IC} decreases with longer aging time. The relaxation/retardation spectrum of this type of networks were modified with the ratio of bimodal molecular weight distribution of curing agent used (i.e. diamine). However, for all networks investigated here, the creep compliance curves and stress relaxation curves at different aging time and aging temperature were able to be superimposed and form master curves, thus demonstrating the applicability of the classical time-aging time; time-temperature superposition principle to each these of networks.

ACKNOWLEDGMENTS

I would like to thank Dr. Andre Lee for his support and guidance in completing this research. Without his ideas, encouragement, constant focusing of my research, and patience this body of work would not have been completed. I would also like to thank to my committee members Dr. Iwona Jasiuk and Dr. Dahsin Liu for their valuable suggestions.

TABLE OF CONTENTS

	Page
LIST OF TABLES	vi
LIST OF FIGURES	vii
CHAPTER 1 INTRODUCTION	1
CHAPTER 2 FRACTURE	
2.1 Introduction	6
2.2 Experimental Procedures	
2.2.1 Materials and Sample Preparation	8
2.2.2 Sample Characterization	11
2.2.3 Physical Aging Condition and Fracture Experiment	12
2.2.4 Data Analysis Method	12
2.3 Results and Discussion	
2.3.1 DSC Results	13
2.3.2 Fracture Experiment Results	21

CHAPTER 3	VISCOELASTIC RESPONSES	
3.1	Introduction	30
3.2	Experimental Procedures	
3.2.1	Materials and Sample Preparation	34
3.2.2	Sample Characterization	36
3.2.3	Physical Aging Experiment	37
3.2.4	Data Analysis Method	39
3.3	Results and Discussion	
3.3.1	DSC Results	41
3.3.2	Creep Compliance Test Results	
3.3.2.1	Boltzmann Superposition	42
3.3.2.2	Aging Results	44
3.3.3	Stress Relaxation Results	
3.3.3.1	Boltzmann Superposition	66
3.3.3.2	Aging Results	66
CHAPTER 4	CONCLUSIONS	77
	REFERENCES	79

LIST OF TABLES

Table 1. Samples for fracture tests

Table 2. DSC Results for fracture tests specimens

Table 3. Fracture toughness result

Table 4. Samples for DGEBA/diamine networks

Table 5. DSC results for the DGEBA/diamine networks

Table 6. The KWW curve fitting parameters of creep compliance tests for $T_g - T = 15^\circ \text{C}$

Table 7. The KWW curve fitting parameters of creep compliance tests for $T_g - T = 8^\circ \text{C}$

Table 8. The KWW curve fitting parameters of creep compliance tests for $T_g - T = 5^\circ \text{C}$

Table 9. The KWW curve fitting parameters of stress relaxation tests for $T_g - T = 15^\circ \text{C}$

LIST OF FIGURES

- Figure 1. Schematic architecture of the DGEBA/PPO networks
- Figure 2. Schematic of enthalpy (volume) versus temperature
- Figure 3. The molecular structure of DGEBA
- Figure 4. The molecular structure of D230, D400 and D2000
- Figure 5. Compact tension configuration and Schematic of the location of fracture surface
- Figure 6. A DSC curve for DGEBA+100%D230
- Figure 7. A DSC curve for DGEBA+99%D230+1%D2000
- Figure 8. A DSC curve for DGEBA+98%D230+2%D2000
- Figure 9. A DSC curve for DGEBA+95%D230+5%D2000
- Figure 10. A DSC curve for DGEBA+98%D230+2%D400
- Figure 11. A DSC curve for DGEBA+95%D230+5%D400
- Figure 12. A DSC curve for DGEBA+90%D230+10%D400
- Figure 13. Critical stress intensity factor K_{IC} as a function of molar ratio of D2000
- Figure 14. Load-displacement for DGEBA/D230 and DGEBA/D230/D2000 after 50 hours aging
- Figure 15. Critical stress intensity factor K_{IC} as a function of aging time for DGEBA/D230 and DGEBA/D230/D2000
- Figure 16. Fracture surface of DGEBA+100%D230 aged for 50 hours
- Figure 17. Fracture surface of DGEBA+98%D230+2%D2000 aged for 50 hours

- Figure 18. Fracture surface of DGEBA+95%D230+5%D2000 aged for 50 hours
- Figure 19. Schematic of volume-temperature plot show volume change from point A to point B during aging
- Figure 20. Schematic of the relative effects of aging on viscoelastic response at point A and point B
- Figure 21. Schematic of stress history where all probes are of equal magnitude
- Figure 22. The response of DGEBA+100%D230 aged at 78.5° C for 24 hours to loading followed by unloading
- Figure 23. Creep compliance curves of DGEBA+100%D230 aged at 66.9±0.3° C for various aging times
- Figure 24. Creep compliance curves of DGEBA + 98%D230 + 2%D2000 aged at 61.1±0.3° C for various aging times
- Figure 25. Creep compliance curves of DGEBA + 95%D230 + 5%D2000 aged at 49.6±0.3° C for various aging times
- Figure 26. Creep compliance curves of DGEBA + 95%D230 + 5%D2000 aged at 49.5±0.3° C for different stress histories
- Figure 27. Creep compliance curves of DGEBA + 100%D230 aged at 75.2±0.3° C for various aging times
- Figure 28. Creep compliance curves of DGEBA + 98%D230 + 2%D2000 aged at 66.6±0.3° C for various aging times
- Figure 29. Creep compliance curves of DGEBA + 95%D230 + 5%D2000 aged at 58.0±0.3° C for various aging times
- Figure 30. Creep compliance curves of DGEBA + 90%D230 + 10%D400 aged at 66.7±0.3° C for various aging times
- Figure 31. Creep compliance curves of DGEBA + 100%D230 aged at 78.5±0.3° C for various aging times
- Figure 32. Creep compliance curves of DGEBA + 98%D230 + 2%D2000 aged at 71.3±0.3° C for various aging times

- Figure 33. Creep compliance curves of DGEBA + 95%D230 + 5%D2000 aged at $60.8 \pm 0.3^\circ \text{C}$ for various aging times
- Figure 34. Creep compliance curves of DGEBA+98%D230+2%D2000 at aging time of 60 min for various aging temperature
- Figure 35. Creep compliance curves of DGEBA+95%D230+5%D2000 at aging time of 60 min for various aging temperature
- Figure 36. Double logarithmic plot of aging time shift factor a_{te} versus aging time for creep compliance test at temperature $T_g - 15^\circ \text{C}$
- Figure 37. Double logarithmic plot of aging time shift factor a_{te} versus aging time for creep compliance test at temperature $T_g - 8^\circ \text{C}$
- Figure 38. Double logarithmic plot of aging time shift factor a_{te} versus aging time for creep compliance test at temperature $T_g - 5^\circ \text{C}$
- Figure 39. The response of DGEBA+98%D230+2%D2000 aged at 60.8°C for 4 hours to loading followed by unloading
- Figure 40. Stress relaxation curves of DGEBA+100%D230 aging at $67.9 \pm 0.3^\circ \text{C}$ for a period of time
- Figure 41. Stress relaxation curves of DGEBA+98%D230+2%D2000 aging at $60.8 \pm 0.3^\circ \text{C}$ for a period of time
- Figure 42. Stress relaxation curves of DGEBA+95%D230+5%D2000 aging at $51.2 \pm 0.3^\circ \text{C}$ for a period of time
- Figure 43. Stress relaxation curves of DGEBA+90%D230+10%D400 aging at $61.0 \pm 0.3^\circ \text{C}$ for a period of time
- Figure 44. Stress relaxation curves of DGEBA+95%D230+5%D2000 at aging time of 480 min for various aging temperature
- Figure 45. Double logarithmic plot of aging time shift factor a_{te} versus aging time for stress relaxation test at temperature $T_g - 15^\circ \text{C}$
- Figure 46. Logarithmic of temperature shift factor a_T versus temperature difference $T - T_g$ for DGEBA+95%D230+5%D2000 at aging time 480 min

CHAPTER 1 INTRODUCTION

In order to elucidate the effect of the molecular weight distribution between crosslinks on the mechanical responses of epoxy networks, difunctional amine terminated curing agent with the same composition but different molecular weight were mixed with diepoxy to form networks of crosslink distribution. The diamines used in this study were linear diamines of poly(propylene oxide) (PPO). As shown in Figure 1. the DGEBA is connected with PPO chain to form varying crosslink density distribution. The DGEBA regularly alternating blocks with diamines formed the crosslinked epoxy networks. The term “alternating” refers to the connection between the long-chain and the short-chain blocks [1].

Glassy polymers are prone to brittle fracture. To improve the fracture toughness, one often incorporates a second rubber phase. This can be accomplished by either add in second rubber phase or directed copolymerization of networks with soft segments (larger distance between crosslink junctions). Although a lot of work have been studied with rubber toughened system, relatively few studies involve copolymerization method. The highly crosslinked thermoset polymer such as epoxy exhibits relatively low resistance to crack propagation. To improve this, one often incorporates second rubbery phase. This is accomplished either by adding a CTBN rubber - the true secondary phase or by incorporating into network with longer distance between crosslink junction. There is a large number of studies which involve rubber toughened epoxy network, while relatively

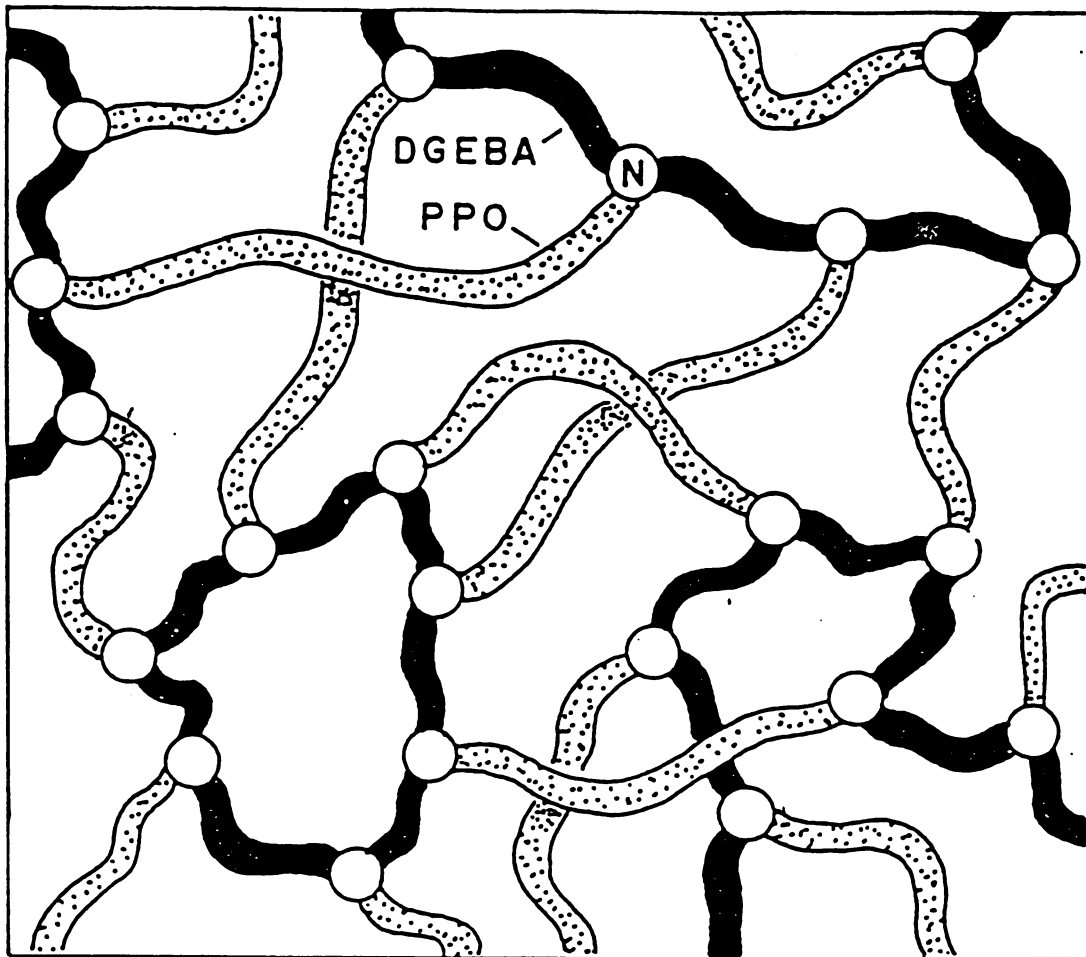


Figure 1. Schematic architecture of the DGEBA/PPO networks

little has been done using copolymerization method. One of the copolymerization methods incorporates diamines with longer molecular weight between crosslink junctions through copolymerization.

In this study, I am particularly interested in the long term performance of these networks. Physical aging is a phenomenon that has recently been shown to have a great importance in considering the long term mechanical behavior of glassy polymers [2]. Physical aging is a result of slow continuation below the glass transition temperature, T_g , of the glass formation process that begins at T_g . After the (kinetic) transition from liquid-like to glass-like behavior, the material is in a non-equilibrium state and its structure spontaneously evolves towards equilibrium [3,4]. Accompanying the change in glassy structure is the change in the mechanical (viscoelastic) response of the glass [5-8].

As the polymer material is cooled through the glass transition, the molecules are essentially "frozen" into a nonequilibrium state relative to the corresponding equilibrium state extrapolated from liquid state; see Figure 2. The glassy state is a unstable thermodynamic state. Therefore, enthalpy and volume of this system spontaneously evolved toward to equilibrium state. The molecular mobility below the glass transition, although greatly reduced, remains finite, thus the physical and mechanical properties of polymers will change with time [9]. Practical interest in the aging behavior of glassy polymer has arisen due to the rather significant mechanical property changes which have been observed to occur as a result of the approach toward the equilibrium state [10,11]. Typical of these changes are an increase in tensile and flexural yield stresses, a decrease in impact strength, fracture energy, ultimate elongation, and creep rate, and a transition

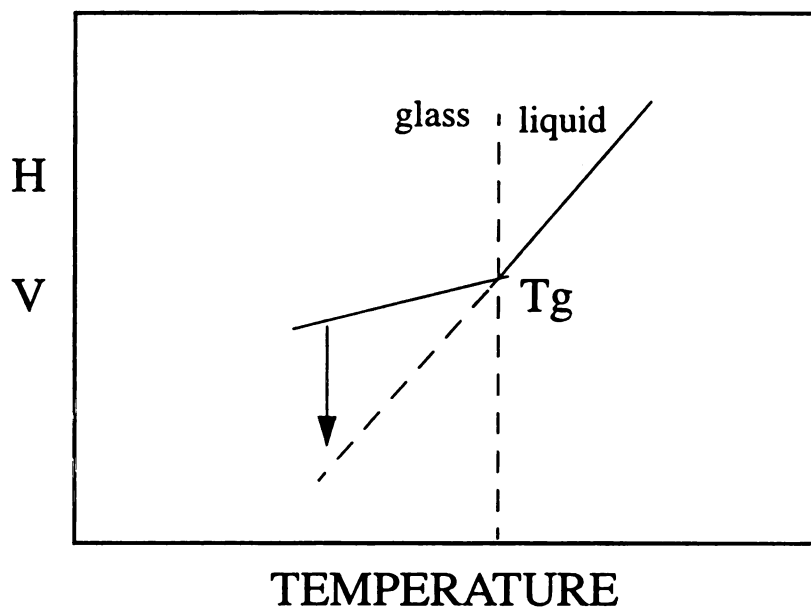


Figure 2. Schematic of enthalpy (volume) versus temperature plot. Arrow showing enthalpy (volume) decrease represents normal isothermal response of a glass after rapid cooling to a non-equilibrium state

from ductile behavior to brittle fracture [12-14]. Such studies have been performed in order to develop a better understanding of the molecular origin of the physical properties in polymers. From these studies, the mechanism of physical aging has been related to molecular conformation, entanglement networks, and free volume [15-18]. Since the behavior of epoxy glasses exhibits both viscous and elastic behavior, they are termed viscoelastic. The examination of this behavior will determine how a polymer will respond to a stress or strain over a long period time at temperature below its T_g . The above factors will lead to an examination of creep compliance and stress relaxation behavior of the epoxy glasses. In particular, how does the crosslink density distribution on mechanical response affect the aging behavior of the epoxy glass? Therefore, fracture and viscoelastic tests can be performed in order to identify the mechanical responses of the epoxy glasses during physical aging. Fracture tests based on compact tension specimen (CTS) and creep compliance and stress relaxation tests in uniaxial extension are performed to characterize the mechanical responses during the aging process.

CHAPTER 2 FRACTURE

2.1 Introduction

Epoxy resins are some of the most commonly used thermosetting polymers. The use of polymer matrix fibrous composites in automotive, durable goods, and infrastructure areas have been slowed by a certain lack of confidence in their durability, reliability and, hence, their cost effectiveness. Among many desirable properties of these networks are high modulus and good performance at elevated temperatures. However, they exhibit poor fracture toughness and low resistance to crack growth [19, 20]. To improve the toughness of glassy polymer, one can incorporate rubber domains into the system. There are two general methods of adding this rubber domain. The first is through blending an incompatible rubbery polymer with the matrix and the second is through copolymerization [21].

The use of rubber particles in a brittle polymer has a major effect upon the mechanical properties. The material will yield and then deform plastically before fracture. Brittle network polymers such as epoxy can be toughened by the addition of a rubbery particles. An example of this is the addition of 8.7% by weight of a carboxyl-terminated poly(butadiene-co-acrylonitrile) (CTBN) rubber to the epoxy prepolymer and curing agent. The rubber is first soluble in the prepolymer mixture but precipitates in the form of particles as the resin increases in molar mass during curing. This volume of precipitate is what controls the toughness of the material [21]. The rubber particles have

a Young's modulus of about 3 orders of magnitude lower than that of the glassy matrix. This causes stress concentration at the equators of the particles during mechanical deformation. Since rubber particles can undergo large elastic deformation, the stress concentration can cause shear yielding or crazing around every particle and hence throughout a large volume of material rather than just at the crack tip. The polymer is toughened by the large amounts of energy absorbed during deformation.

Although rubber toughening is an effective method to improve fracture toughness of polymers, in some applications this phase separation may not be desirable, as for example the phase-separated material is often nontransparent [22]. As an alternative approach to this goal, one incorporated diamines with longer molecular weight between crosslink junctions through copolymerization. Although these methods of toughening are not as effective as compared to rubber toughening, samples remain transparent, and one can achieve high fracture toughness. Since the chain length between crosslink junctions is longer and therefore it takes longer to deform. As mentioned previously, I am interested in the long-term performance of epoxy glasses, the fracture toughness test used in this study was that of the compact tension specimen (CTS) which was aged at 70° C with aging time range from 1 hour to 100 hours. The fracture occurred at room temperature immediately after aging condition. By comparing the results of these tests, the effect of the crosslink density distribution on crosslinked epoxy glasses due to physical aging was determined.

2.2 Experimental Procedures

2.2.1. Materials and Sample Preparation

Diglycidyl ether of bisphenol A (DGEBA, DER 332, Dow Chemical, USA) was chosen as the model epoxy monomer in this work. DGEBA is a difunctional epoxy, the DER332 is typically used commercial epoxy resin.

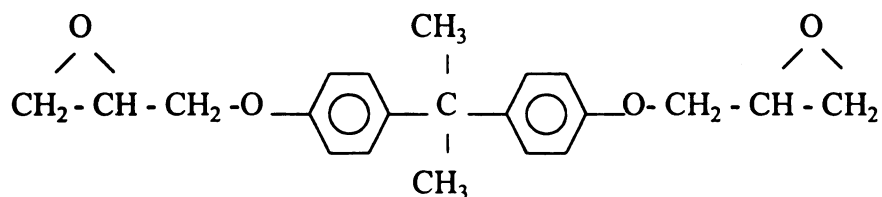


Figure 3. The molecular structure of DGEBA.

Jeffamine of different molecular weight was the curing agent. (Jeffamine is a tradename of Texaco Chemical Company). Jeffamine D230 and D2000 were used in this work. The D-series amines are difunctional amines linked by poly(propylene oxide) (PPO) chain. Where n is the average number of repeat units in the epoxy resin molecule. (The number of n is taken from manufacture's booklet).

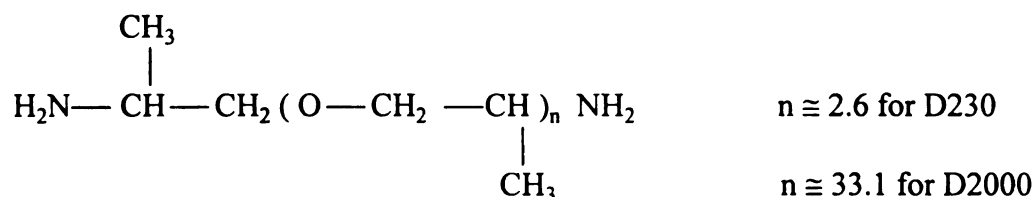


Figure 4. The molecular structure of D230 and D2000.

The DGEBA epoxide monomer was preheated at 60° C for 2 hours to melt any crystals present before hand mixing with the amines until the mixture was clear. The mole ratio of the DGEBA epoxide monomer and amine was that of the stoichiometric ratio. The mixture was degassed for 20 min at room temperature to remove the bubbles, then cast into a mould with dimensions of 8 x 4 x 0.25 inch (20.32 x 10.16 x 0.635 cm) and cured at 100° C for 24 hours. The sample was then allowed to cool slowly in the oven overnight to 23° C. Specimens conforming to ASTM D5045-91 geometry (a = 0.35 inch (0.89 cm), B = 0.25 inch (0.64 cm) and W = 1.00 inch (2.54 cm) were machined from the cast sheets (The dimensions are shown in Figure 5). The samples were kept in a sealed desiccator until the experiments were performed.

All the samples were cured with stoichiometric amounts of reactants, i.e., one mole of diamine to two moles of epoxy resin. The molar ratio of diepoxide to diamine was kept in stoichometric ratio, i.e. [E] : [H] = 1 : 1 (see Table 1). The following is the example calculation used to convert number fraction to weight fraction for DGEBA, D230 and D2000.

$$\text{DGEBA} = (340 \text{ g / mol }) / 2 \text{ epoxy groups} = 170 \text{ g / epoxy group (eg)}$$

$$\text{D230} = (230 \text{ g / mol }) / 4 \text{ amine groups} = 57.5 (\text{ g / eg })$$

$$\text{D2000} = (2000 \text{ g / mol }) / 4 \text{ amine groups} = 500 (\text{ g / eg })$$

Example calculation: DGEBA + 100%D230

$$(1) * (57.5 \text{ g / eg }) + 170 (\text{ g / eg }) = 227.5 (\text{ g / eg })$$

$$\text{Weight fraction of D230} = (57.5 \text{ g / eg }) / (227.5 \text{ g / eg }) = 0.2527$$

$$\text{Weight fraction of DGEBA} = (170 \text{ g / eg }) / (227.5 \text{ g / eg }) = 0.7473$$

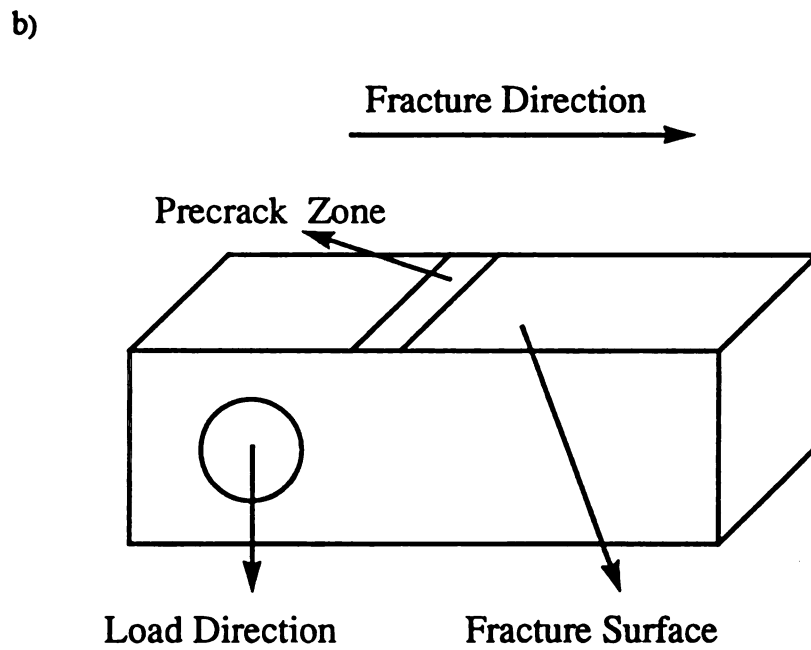
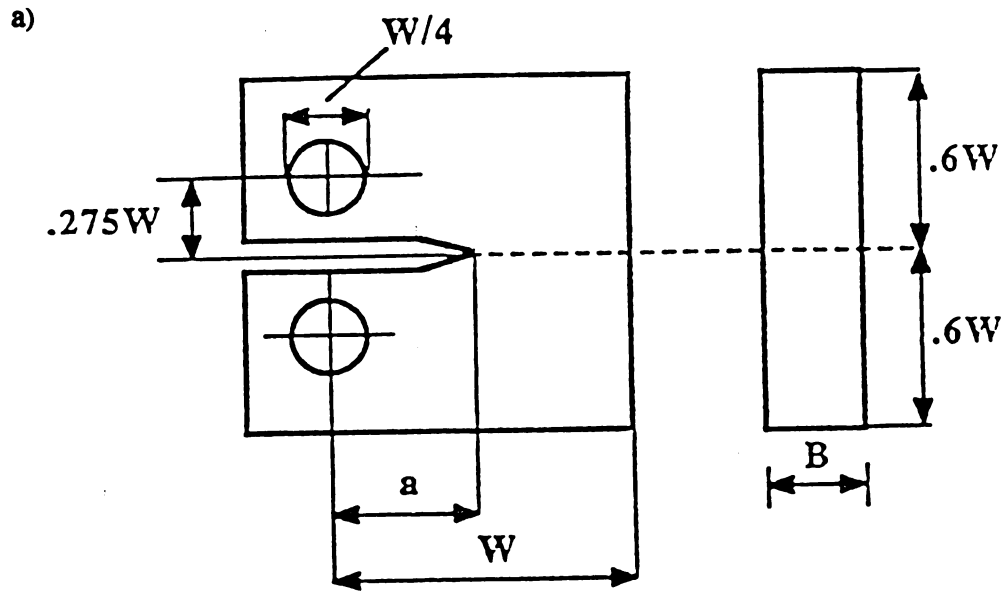


Figure 5. a) Compact Tension Configuration
b) Schematic of the location of fracture surface

Table 1: Samples for fracture tests

Sample	Molar ratio* of [E] : [H] _{D230} : [H] _{D2000}
A : DGEBA+100%D230	1 : 1 : 0
B: DGEBA+98%D230+2%D2000	1 : 0.98 : 0.02
C: DGEBA+95%D230+5%D2000	1 : 0.95 : 0.05

*[E]: Epoxide monomer

[H]_{D230}: Hydrogen contributed by D230

[H]_{D2000}: Hydrogen contributed by D2000

2.2.2. Sample Characterization

The TA Instruments Differential Scanning Calorimeter (Modulated DSC) 2920 applies an enthalpy-change method to determine the difference in energy flow into a material as a function of temperature. These measurements are all taken in relationship to a reference material under a controlled temperature program. The glass transition temperature is where an amorphous solid becomes rubbery. The glass transition is accompanied by a change in heat flow of the sample and therefore will be indicated on the DSC curve.

The glass transition temperature, T_g , and the changes in heat capacity ΔC_p at T_g for the testing samples were determined by the MDSC. The temperature scale was calibrated with the melting transition of indium. Temperature scans were performed at $5^\circ \text{C}/\text{min}$ with modulated $\pm 1^\circ \text{C}$ every 60 seconds and was operated over a temperature ranging from -60°C to $+120^\circ \text{C}$. Tests were performed on 10 to 20 mg samples. The heating scans were performed immediately after cooling samples which had been held at

120° C for 30 min to erase the thermal history. The T_g was taken by the inflection point, the point on the curve with the steepest slope, which is considered the midpoint of the step transition from glassy to the liquid state.

2.2.3. Physical Aging Condition and Fracture Experiment

All the specimens were first annealed at 102° C (20° C above T_g of DGEBA/D230) for 30 minutes to remove all previous aging. Immediately after annealing, all the specimens were put into the oven and held at 70° C for aging. The aging time ranged from 1 to 100 hours. Immediately after aging treatment, the machine notched specimens were precracked to approximately 0.2 inches. The precracking procedure consisted of placing a razor blade dipped in liquid nitrogen and tapping it with a hammer. The fracture measurements were then performed using a computer-controlled screw-driven testing machine (Instron apparatus model 4206) at room temperature and at crosshead speed of 10 mm/min. A loading clevis suitable for testing compact tension specimens is used to clip the test specimen. Both ends of the specimen are held in such a clevis and loads are applied to the sample through the pins. An Olympus reflected/transmitted light microscope with camera attachment was used to analyze of the CTS fracture surface morphology.

2.2.4 Data Analysis Method

All the fracture toughness data were analyzed according to the concepts of linear elastic fracture mechanics (LEFM) [23]. The critical stress intensity factor K_{IC} , is also

called the fracture toughness because it characterizes the resistance of a material to crack propagation. It is normally a function of the applied load, crack length and specimen dimensions. According to ASTM D 5045-91 the following formulas were used to calculate the K_{IC} factor.

$$K_Q = (P_Q / BW^{1/2}) f(X) \quad (1)$$

where ($0.2 < X < 0.8$):

$$f(X) = [(2 + X)(0.886 + 4.64X - 13.32X^2 + 14.72X^3 - 5.6X^4)] / (1 - X)^{3/2}$$

P_Q = the maximum tensile load

B = the thickness of the specimen

W = the width of the specimen

a = the initial crack length of the specimen

$$X = a / W$$

2.3 Results and Discussion

2.3.1 DSC Results

The DSC results for DGEBA/D230 and a blend containing 2% and 5% of D2000 are presented in Table 2 and Figure 6, Figure 8 and Figure 9. All the materials exhibit a primary transition zone corresponding to the glass transition temperature (T_g). One can see that as the amount of D2000 increase, the glass transition temperature (T_g) is decreased, the heat capacity (C_p) at T_g is increased, the glass transition zone is considerably broadened as increasing the amount of D2000. Because the T_g 's of the two components (DGEBA/D230 is 82.89° C, and DGEBA/D2000 is -48° C) are not close, the

Sample: DGEBA+100%D230

Size: 12.5000 mg

Method: MOD. RAMP -60 TO 140°C

Comment: MOD. RAMP AT 5°C/MIN. -60°C TO 140°C

DSC

File: C: 100%D230.005

Operator: YTW

Run Date: 3-Jan-95 17:32

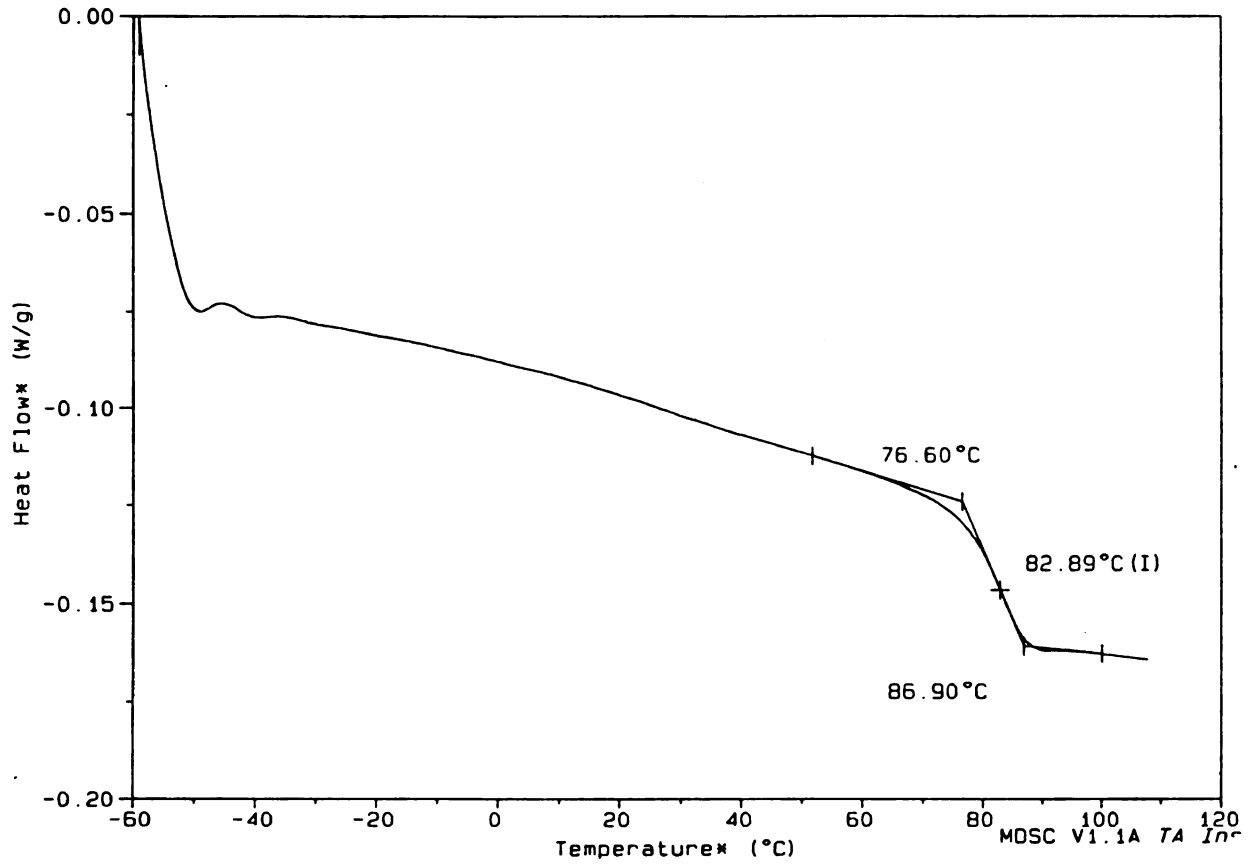


Figure 6. A DSC curve for DGEBA + 100%D230

Sample: DGEBA+99%D230+1%D2000

Size: 13.8000 mg

Method: MOD. RAMP -60 TO 120°C

Comment: MOD. RAMP AT 5°C/MIN. -60°C TO 120°C, SECOND RUN

DSC

File: C:\1\02000.002

Operator: YTW

Run Date: 4-Jan-95 23:44

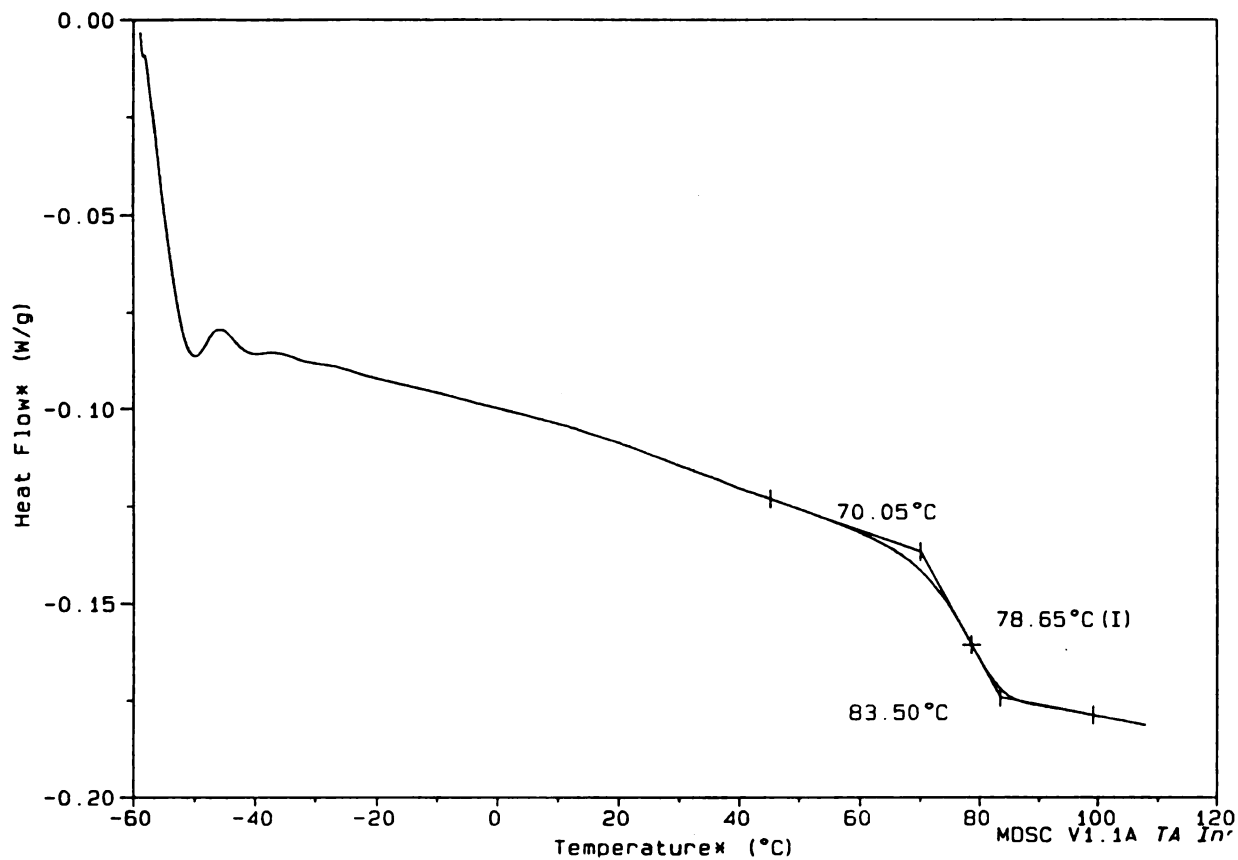


Figure 7. A DSC curve for DGEBA + 99%D230 + 1% D2000

Sample: DGEBA+98%D230+2%D2000
Size: 12.7000 mg
Method: MOD. RAMP -60 TO 120°C
Comment: MOD. RAMP AT 5°C/MIN, -60°C TO 120°C, SECOND RUN

DSC

File: C:\2\02000.002
Operator: YTW
Run Date: 4-Jan-95 21:17

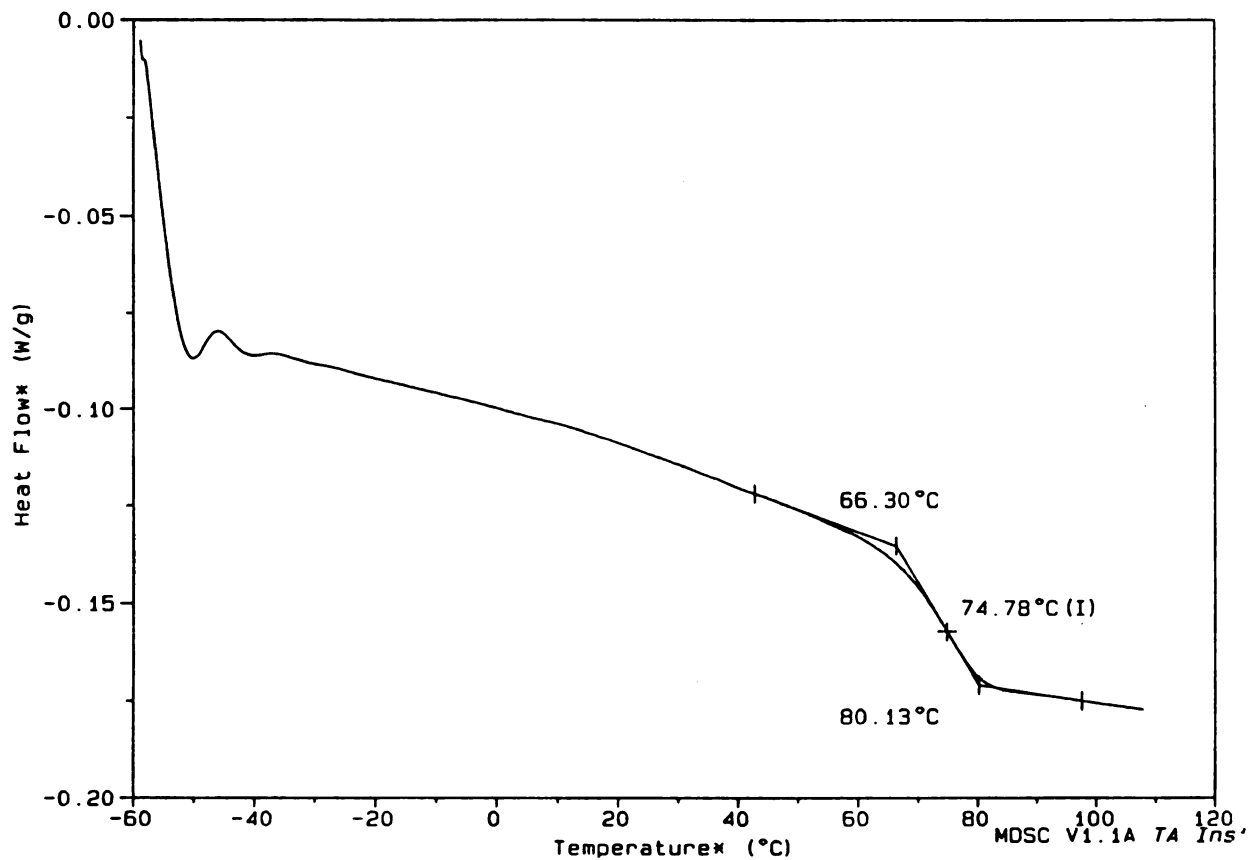


Figure 8. A DSC curve for DGEBA + 98%D230 + 2%D2000

Sample: DGEBA+95%D230+5%D2000
Size: 11.3000 mg
Method: MOD. RAMP -60 TO 120°C
Comment: MOD. RAMP AT 5°C/MIN. -60°C TO 120°C, SECOND RUN

DSC

File: C: 5%D2000.002
Operator: YTW
Run Date: 3-Jan-95 22:57

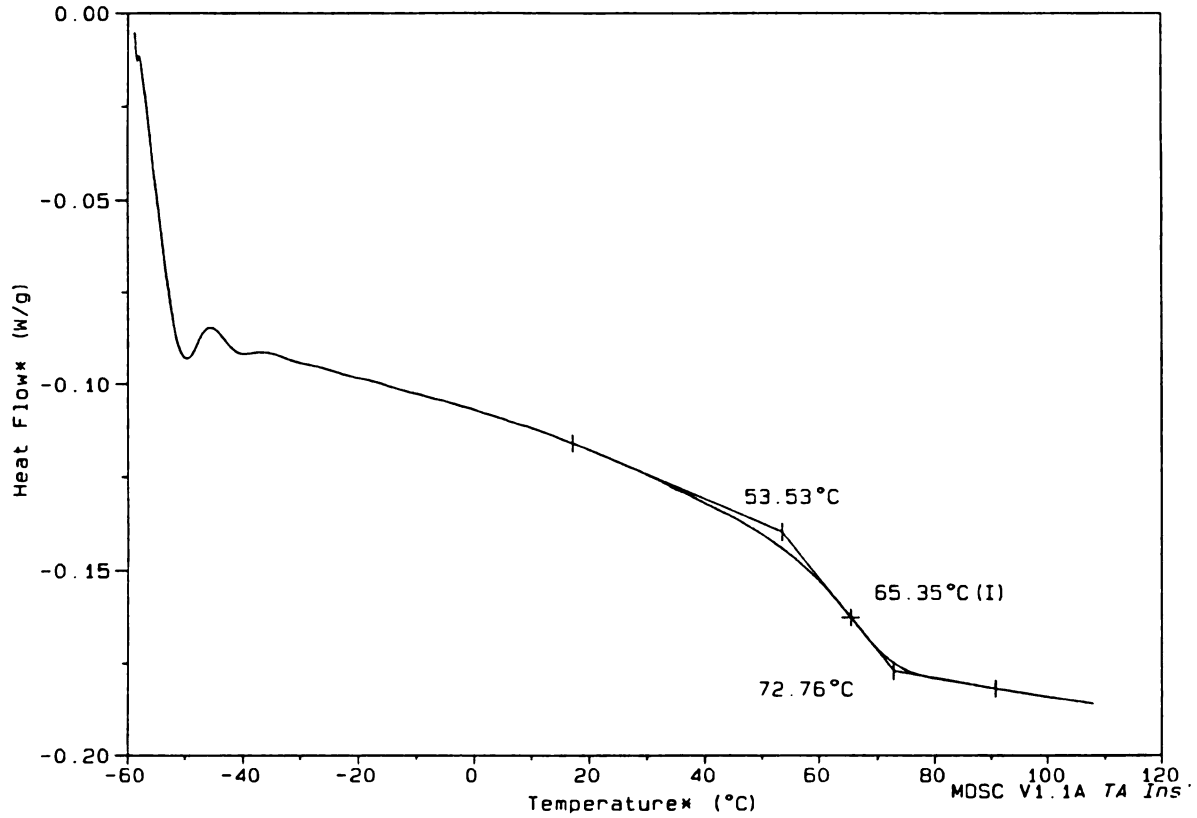


Figure 9. A DSC curve for DGEBA + 95%D230 + 5%D2000

Sample: DGEBA+98%D230+2%D400
Size: 13.5000 mg
Method: MOD. RAMP -60 TO 120°C
Comment: MOD. RAMP AT 5°C/MIN, -60°C TO 120°C SECOND RUN

DSC

File: C:2%D400.002
Operator: YTW
Run Date: 10-Jan-95 02:23

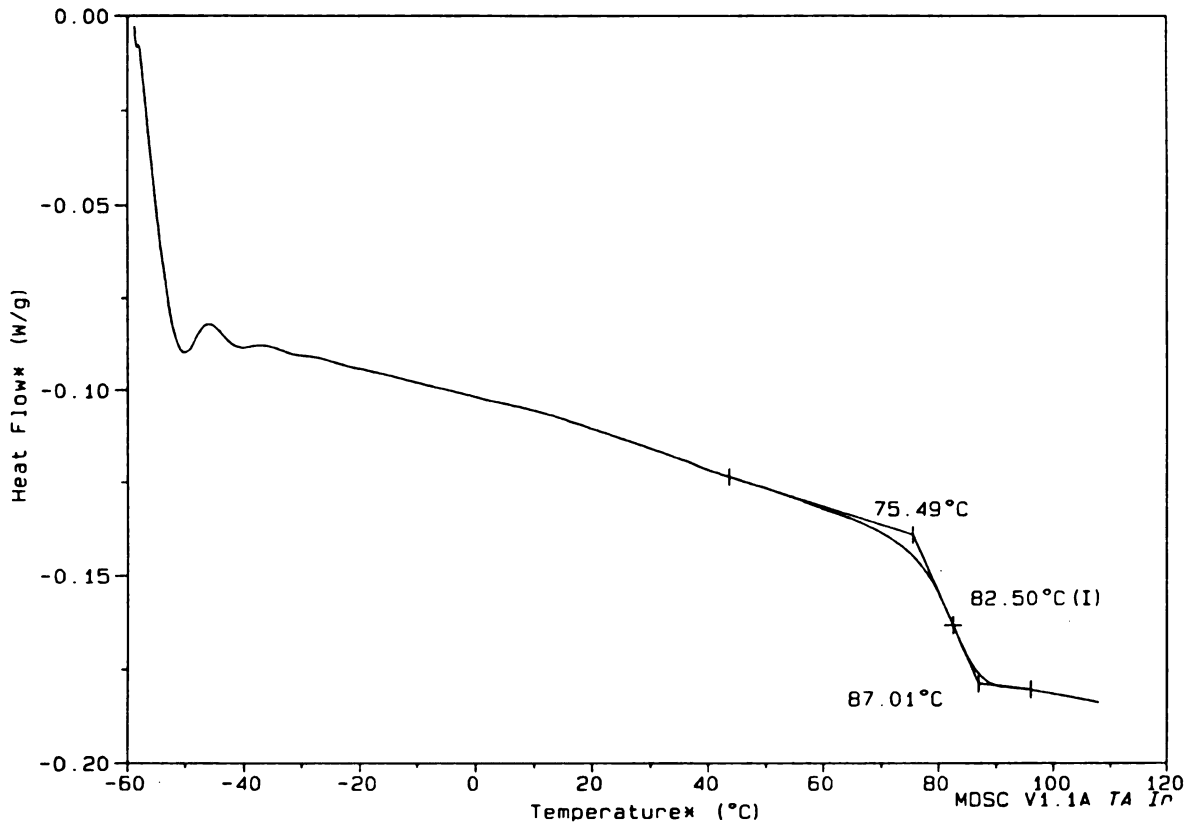


Figure 10. A DSC curve for DGEBA + 98%D230 + 2%D400

Sample: DGEBA+95%D230+5%D400

Size: 12.9000 mg

Method: MOD. RAMP -60 TO 120°C

Comment: MOD. RAMP AT 5°C/MIN. -60°C TO 120°C SECOND RUN

DSC

File: C: 5%D400.002

Operator: YTW

Run Date: 10-Jan-95 04:46

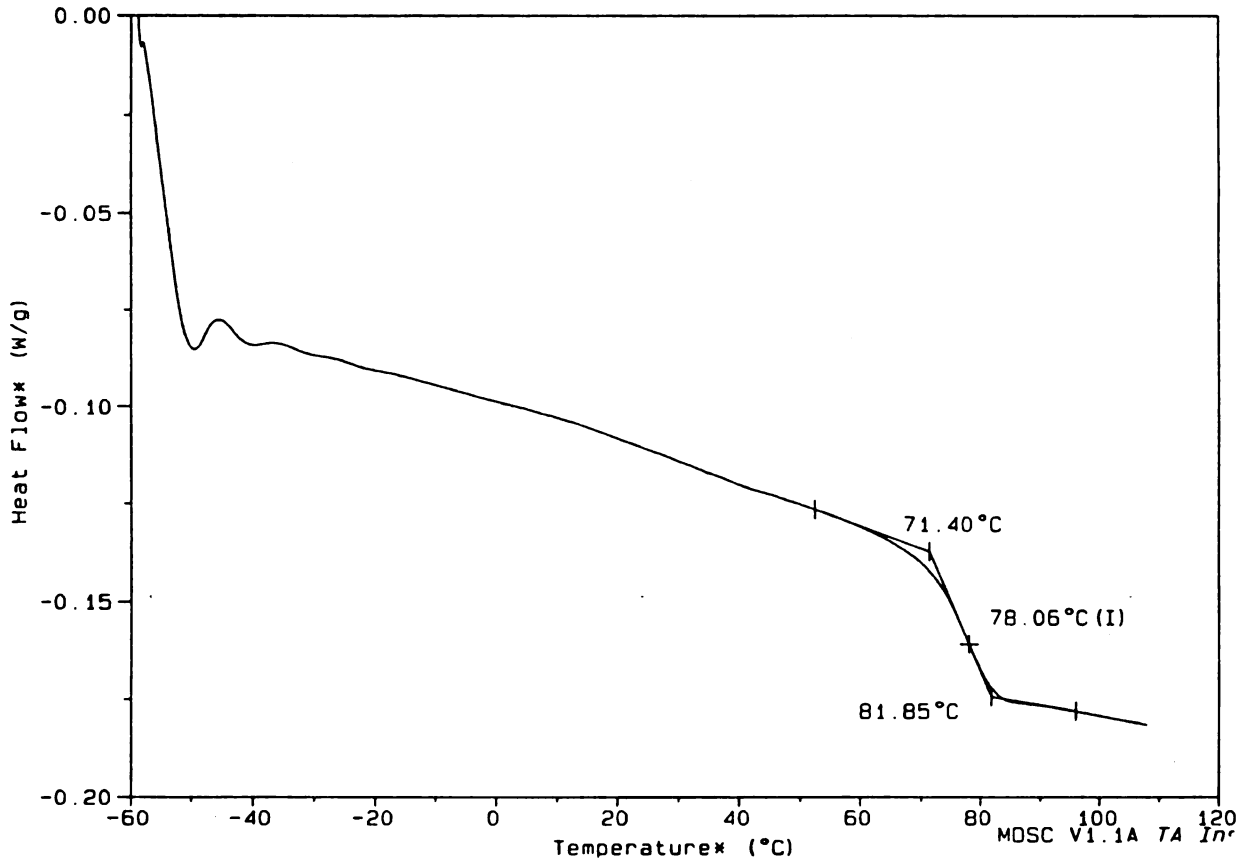


Figure 11. A DSC curve for DGEBA + 95%D230 + 5%D400

Sample: DGEBA+90%D230+10%D400

DSC

File: C: 10%D400.002

Size: 12.1000 mg

Operator: YTW

Method: MOD. RAMP -60 TO 120°C

Run Date: 10-Jan-95 20: 43

Comment: MOD. RAMP AT 5°C/MIN, -60°C TO 120°C SECOND RUN

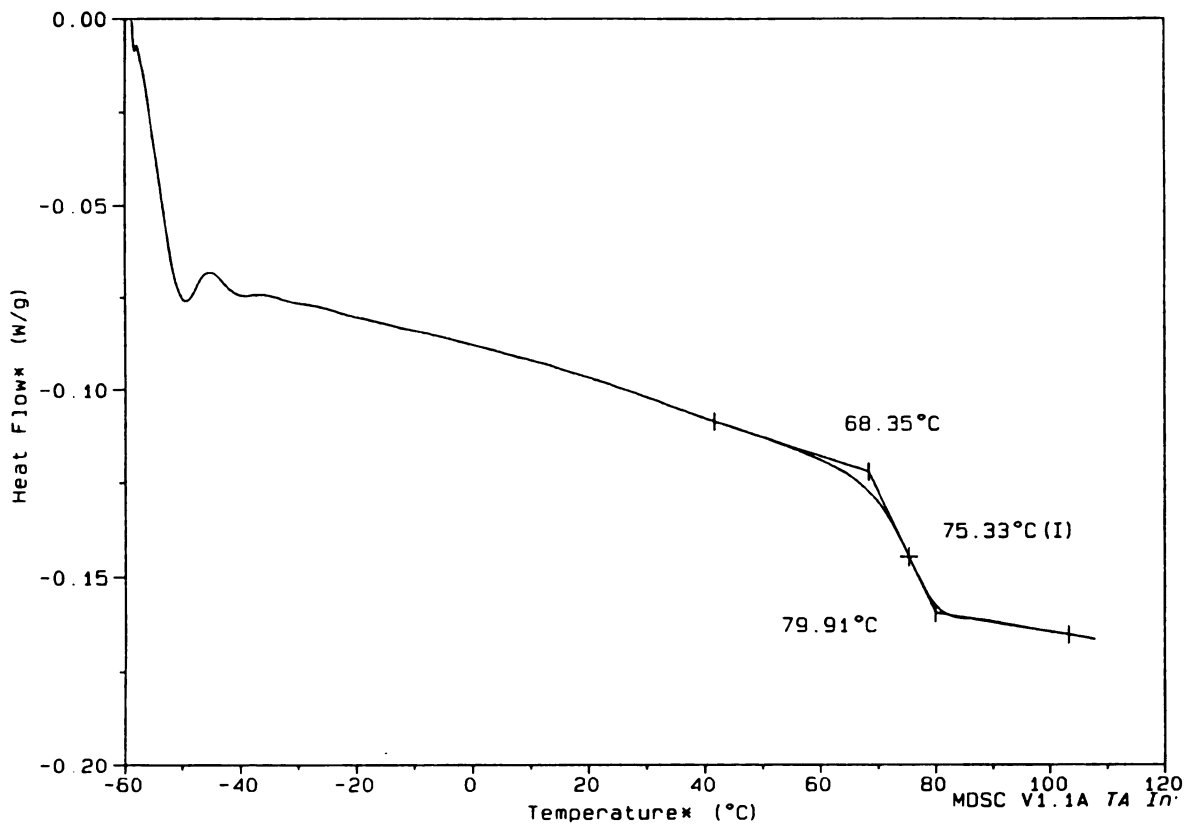


Figure 12. A DSC curve for DGEBA + 90%D230 + 10%D400

temperature range of DSC curve is from -60°C to $+120^{\circ}\text{C}$. Since there is only one glass transition temperature for each specimen, the above observations indicated that no phase separation has occurred when blending the small amount of D2000. It is apparent that the epoxy network is still a single phase network. The components of each specimen are compatible each other. But by adding the D2000, the glass transition zone is broader, which indicates where the system has broadened crosslink distribution.

Table 2. DSC Results

Sample	T _g (°C)	ΔC_p (J/g/°C)	Glass Transition Zone (°C)
A	82.89	0.1208	10.30
B	74.78	0.1343	13.83
C	65.35	0.1370	19.23

2.3.2 Fracture Experiment Results

The fracture behavior of epoxy glass networks has been examined. The calculated critical stress intensity factor K_{IC} , determined from the load-displacement curves according to eqn. (1) is reported in Table 3.

Table 3. Fracture toughness result, K_{IC} (MPa m^{1/2})

Sample	K_{IC} , at different aging time		
	1 hour	50 hours	100 hours
A: DGEBA +100%D230	0.84±0.08	0.92±0.09	0.96±0.08
B: DGEBA + 98%D230 + 2%D2000	1.15±0.10	1.15±0.07	1.14±0.12
C: DGEBA + 95%D230 + 5%D2000	1.27±0.11	1.60±0.09	1.56±0.09

The value of critical stress intensity factor K_{IC} is reported in Figure 13. as a function of the molar ratio of D2000 in the blend after 1 hour physical aging. It will noted that there is a significant increase in K_{IC} with increasing D2000 content. It demonstrated an correlation between K_{IC} and the amount of D2000 in the blend. This results are the same as a single phase homogeneous epoxy/polycarbonate network, i.e., the fracture toughness of this blend system increases marketly with increasing PC content in the blend [24]. The toughening effect of D2000 is more dramatically evidenced on Figure 14. The curve shown in Figure 14 is observed for the unmodified and D2000 modified epoxy resin after 50 hours aging. In curve A and B, the load rises linearly with strain up to maximum value where the crack propagates instantaneously causing a rapid drop in the load. The corresponding fracture surface exhibits a smooth and relatively featureless surface which can be evidence of brittle failure in Figures 16 and 17. The load-displacement curve shown in Figure 14C is representative of blend containing 5% of D2000. The load increases linearly up to a critical value and then the crack propagates intermittently in a stable manner until the stored elastic energy in the sample decreases to such an extent that crack arrest is allowed. Upon reloading the sample the process of crack-growth is iterated up to the complete failure of the sample. Examination of the corresponding fracture surface show clear evidence of ductile failure in Figure 18.

The critical stress intensity factor K_{IC} as a function of aging time is reported in Figure 15. During physical aging, the value of K_{IC} for the sample A and sample B didn't change very much, but sample C containing 5%D2000 had a significant increase with increasing aging time and failed in a ductile manner. This ductile failure is important

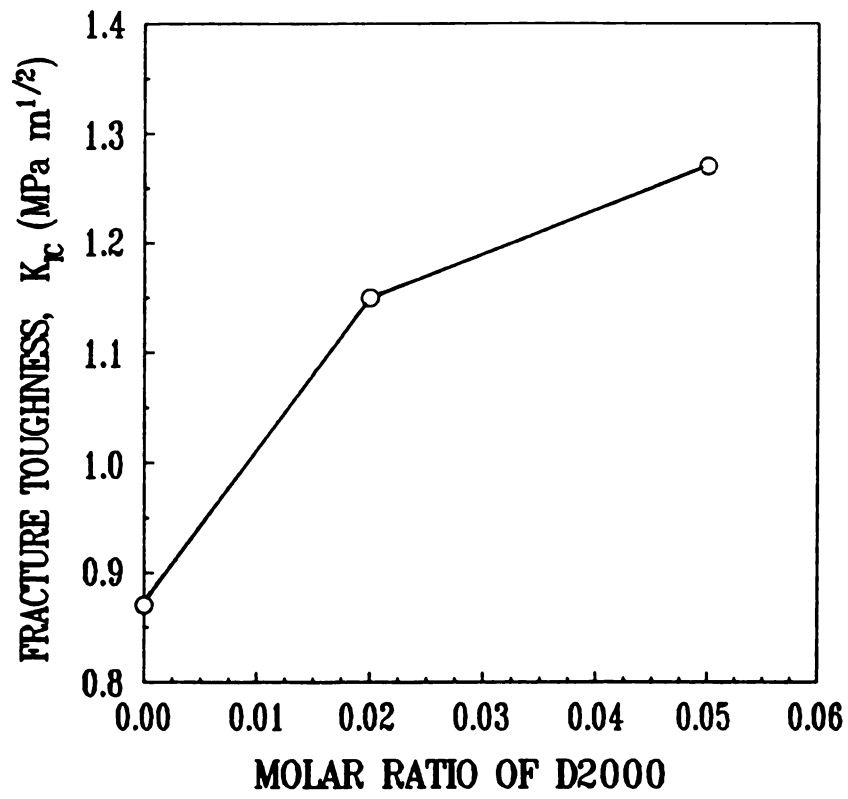


Figure 13. Critical stress intensity factor K_{IC} as a function of molar ratio of D2000 (after 1 hour aging)

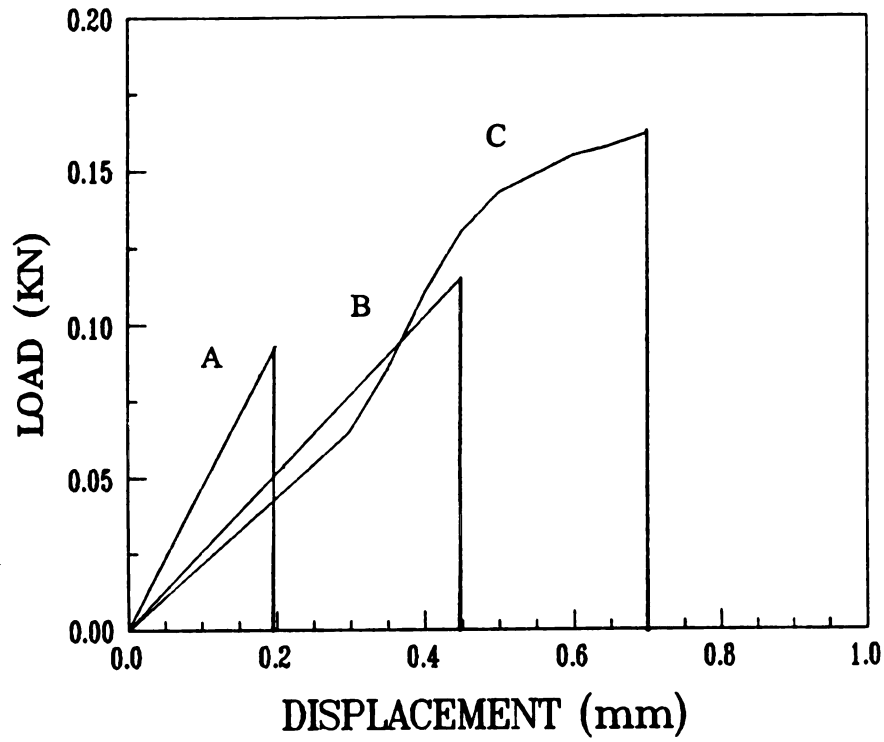


Figure14. Load-displacement curve (after 50 hours aging)

(A) DGEBA + 100%D230; (B) DGEBA + 98%D230
+ 2%D2000; (C) DGEBA + 95%D230 + 5%D2000

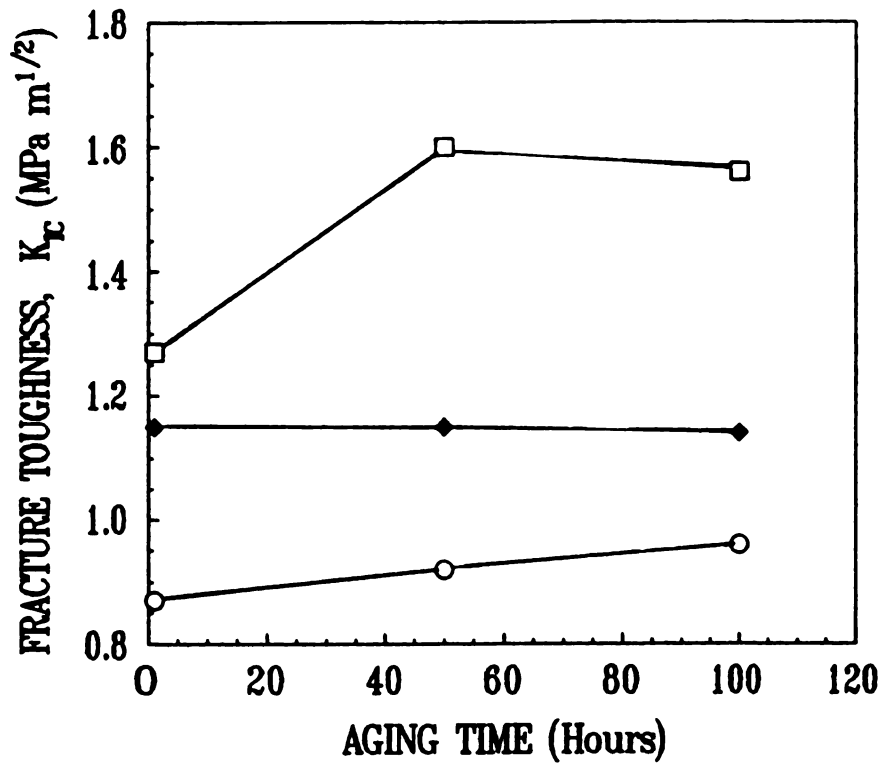


Figure 15. Critical stress intensity factor K_{Ic} as a function of aging time (O) DGEBA + 100%D230; (◆) DGEBA + 98% D230 + 2%D2000; (□) DGEBA + 95%D230 + 5%D2000

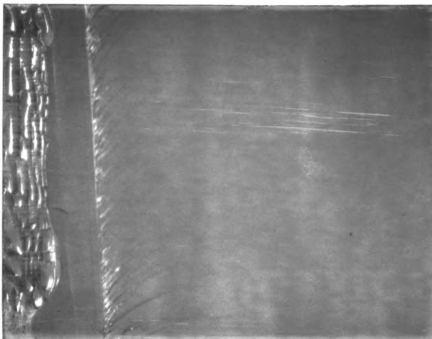


Figure 16. Fracture surface of DGEBA + 100%D230 aged for 50 hours (x 20)

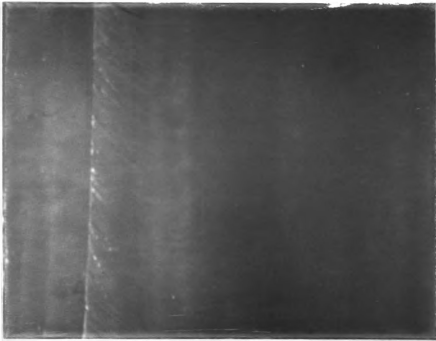


Figure 17. Fracture surface of DGEBA + 98%D230 + 2%D2000 aged for 50 hours (x 20)

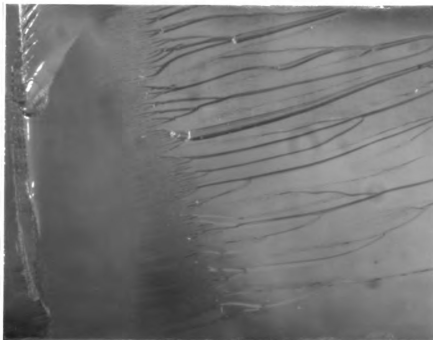


Figure 18. Fracture surface of DGEBA + 95%D230 + 5%D2000 aged for 50 hours (x 20)

because it contradicts characteristics of physical aging in amorphous materials defined by Struik [9] that during the aging material becomes more and more glass-like and less rubber-like. It becomes stiffer and more brittle.

The considerable increase in toughness found in epoxy/diamine can be ascribed to an increase D2000 in the epoxy glasses network. Toughness depends on the distance between crosslinking point in network. Increasing the length of the chain will toughen the cured epoxy. Because the D2000 molecular segments are longer and more flexible than D230, so the D2000 as hardener play a role in increasing the fracture toughness. On a molecular level, physical aging is thought to accompany motion of the polymer chains into a tighter packing density without crystallization [25]. When comparing the three samples, after 1 hour aging, the sample B and sample C have a higher fracture toughness than sample A due to its D2000 content. When the samples aged at 70° C, both sample A and sample B are in glassy state (below their T_g), the fracture toughness didn't change during aging. But for sample C containing 5%D2000, since it is above its T_g for D2000, would generally have a higher molecular mobility than that of the glass phase, which is below T_g. The long and flexible D2000 chains congregate together, this cause the ductile failure at longer aging time.

CHAPTER 3 VISCOELASTIC RESPONSES

3.1 Introduction

A distinctive feature of the mechanical behavior of polymer is the way in which their response to an applied stress or strain depends upon the rate or time period of loading. This dependence upon rate and time is in marked contrast to the behavior of elastic solids such as metals and ceramics which, at least at low strains, obey Hooke's law and the stress is proportional to the strain and independent of loading rate. On the other hand the mechanical behavior of viscous liquids is time dependent. It is possible to represent their behavior at low rates of strain by Newton's law whereby the stress is proportional to the strain rate and independent of the strain. The behavior of most polymers can be thought of as being somewhere between that of elastic solid and viscous liquids. Polymers are therefore termed viscoelastic as they display aspects of both viscous and elastic types of behavior. This leads to a specific relationship between stress and strain. When the strain is held constant and the stress decays slowly with time whereas in an elastic solid it would remain constant, this behavior of a viscoelastic material is referred as stress relaxation. If a constant stress is applied to the specimen at zero time and the strain increases rapidly at first, showing down over longer time periods, this is called creep.

In glass forming polymers, when sample is cooled from above glass transition, the polymer materials are not in thermodynamic equilibrium state at temperature below the

g
v
P
v
c
so
p
ai
vis
a c
vis
The
stre
Eit
and
the
and
the
epox
studie

glass transition, the gradual rearrangement of molecular chains will occur [26, 27]. Volume relaxation studies reveal that below T_g the molecular mobility is not quite zero. There is a slow and gradual approach to equilibrium. During this volume evolution the viscoelastic behaviors of polymer materials also change [6]. Physical aging is the change in viscoelastic properties accompanying the volume relaxation. Example of schematic graph is shown in Figure 19 and Figure 20, where the volume change between point A and point B, the viscoelastic response (creep compliance) will shift horizontally along the time axis.

The viscoelastic response can generally be categorized as linear and nonlinear viscoelastic depending on the type of loading. The Boltzmann superposition principle is a corner-stone of the linear viscoelasticity. It allows the state of stress or strain in a viscoelastic body to be determined from knowledge of its previous deformation history. The basic assumption is that the responses can be determined from the algebraic sum of strains/stress due to each stress/strain step, i.e., $e(t) = \sum \Delta\sigma_i D(t-t_i)$ and $\sigma(t) = \sum \Delta e_i E(t-t_i)$, where $e(t)$ and $\sigma(t)$ are the overall strain and stress from each increment; $D(t-t_i)$ and $E(t-t_i)$ are creep compliance and stress relaxation modulus [21].

According to the time-aging time superposition principle, it is possible to predict the long term properties of polymeric materials using short term tests. Creep compliance and stress relaxation studies can be performed on polymer materials to help understand the dependence of stress and strain upon aging time. The viscoelastic response of the epoxy/diamine networks of different crosslink densities with homogeneous length was studied by Lee and McKenna [5]. In their study, the crosslink density increase with

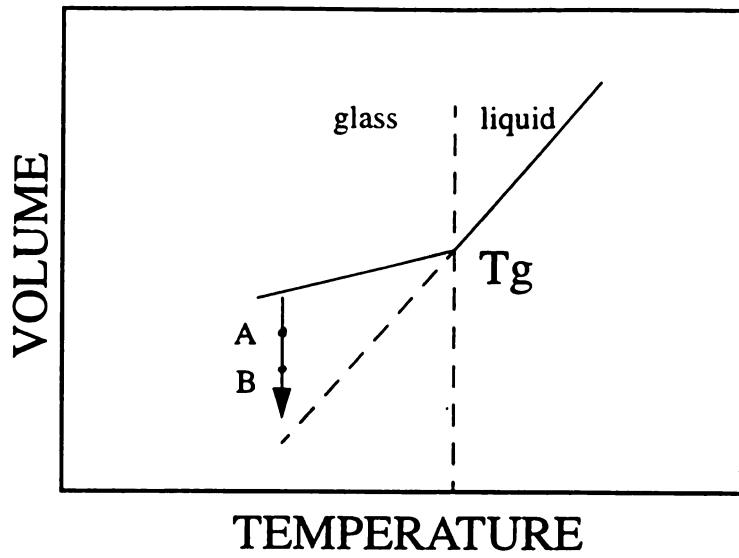


Figure 19. Schematic of volume-temperature plot show volume change from point A to point B during aging

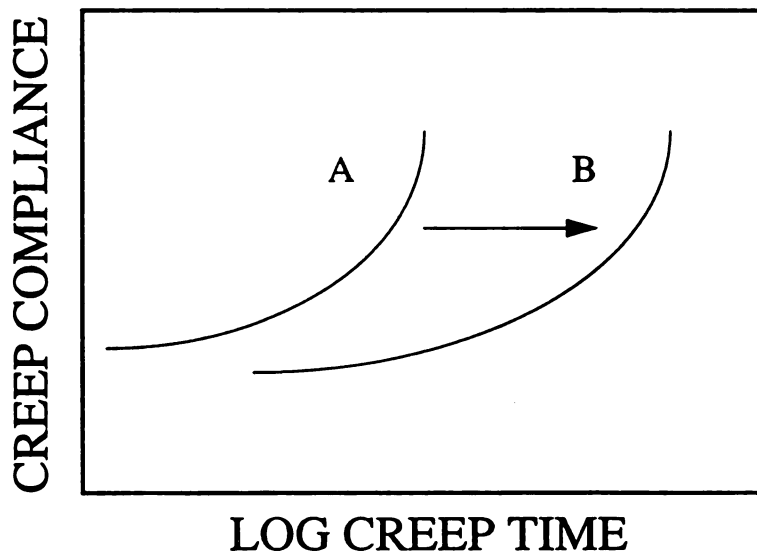


Figure 20. Schematic of the relative effects of aging on viscoelastic response at point A and point B

decrease the length between junctions, it was found that when the crosslink density increases, the glass transition temperature (T_g) increase, but the ΔC_p at T_g didn't change, the shape of the viscoelastic spectrum was also found to be independent of crosslink density for the epoxy networks, and the master curves for different crosslink densities could be superimposed onto a single curve consistent with a time - aging time - temperature - crosslink density superposition principle. Below described work in which the epoxy/diamine networks of different crosslink densities with bimodal length, its network is a random network crosslinked by random junction points. Analysis the data from the creep compliance under small step stress and the small strain stress relaxation tests in simple extension for different aging times and temperatures will show the relationship between the viscoelastic responses and the crosslink density distribution in bimodal length network.

3.2 Experimental Procedures

3.2.1. Materials and Sample Preparation

Two types of epoxy specimens were studied; one contained a single diamine (DGEBA/D230) and the other contained a mixture of two diamines (DGEBA/D230/D2000 or D400). Diglycidyl ether of bisphenol A (DGEBA, DER 332, Dow Chemical, USA) was chosen as the model epoxy monomer in this work.

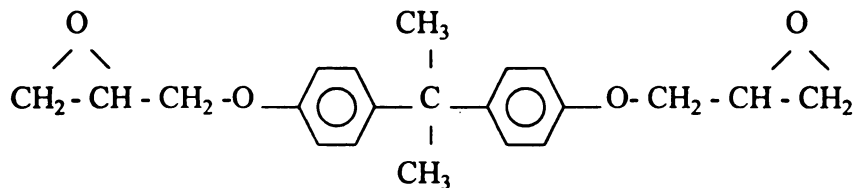


Figure 3. The molecular structure of DGEBA.

Jeffamine of different molecular weight was the curing agent. (Jeffamine is a tradename of Texaco Chemical Company). Jeffamine D230, D400, and D2000 were used. The D-series amines are difunctional amines linked by poly(propylene oxide) (PPO). Where n is the average number of repeat units in the epoxy resin molecule. (The number of n is taken from manufacture booklet).

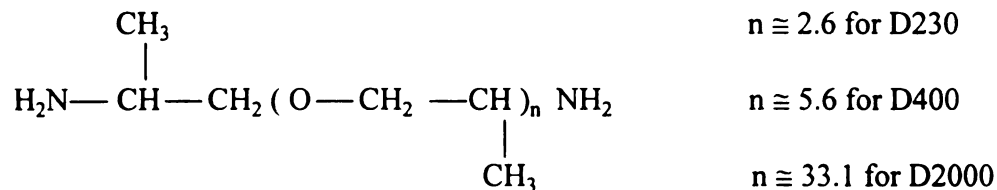


Figure 4. The molecular structure of D230, D400 and D2000.

The DGEBA epoxide monomer was preheated at 60° C for 2 hours to melt any crystals present before hand mixing with the amines until the mixture was clear. The mole ratio of the DGEBA epoxide monomer and hydrogen contributed by D230, D400 and D2000 was that of the stoichiometric ratio. The mixture was degassed for 20 min at room temperature to remove the bubbles, then cast into a mould with dimensions of 6.5 x 0.75 x 0.15 inch (16.51 x 1.91 x 0.38 cm) and cure at 100° C for 24 hours. The sample was then allowed to cool slowly in the oven to 23° C overnight. Specimens conforming to ASTM D638 geometry were machined from the cast sheets, milled into dumb-bell shaped samples. The edges and surfaces of the samples were abraded with 600 grit SiC paper to keep the samples parallel sided thickness, then kept in a sealed desiccator until the experiments were performed.

The following is the calculation used to convert number fraction to weight fraction for DGEBA, D230, D400, and D2000. All the samples were cured with stoichiometric amounts of reactants, i.e., [E] : [H] = 1 : 1 (See Table 4).

$$\text{DGEBA} = (340 \text{ g / mol }) / 2 \text{ epoxy groups} = 170 \text{ g / epoxy group (eg)}$$

$$\text{D230} = (230 \text{ g / mol }) / 4 \text{ amine groups} = 57.5 \text{ (g / eg)}$$

$$\text{D400} = (400 \text{ g / mol }) / 4 \text{ amine groups} = 100 \text{ (g / eg)}$$

$$\text{D2000} = (2000 \text{ g / mol }) / 4 \text{ amine groups} = 500 \text{ (g / eg)}$$

Example calculation: DGEBA + 95%D230 + 5%D2000

$$(0.05) * (500 \text{ g / eg }) + (0.95) * (57.5 \text{ g / eg }) + 170 \text{ (g / eg)} = 249.6 \text{ (g / eg)}$$

$$\text{Weight fraction of D230} = (54.6 \text{ g / eg }) / (249.6 \text{ g / eg }) = 0.2188$$

$$\text{Weight fraction of D2000} = (25.0 \text{ g / eg }) / (249.6 \text{ g / eg }) = 0.1002$$

Wei

A:

B:

C:

D:

E:

F:

G:

H:

I:

J:

3.

ap

ma

a

tem

Weight fraction of DGEBA = (170 g / eg) / (249.6 g / eg) = 0.6810

Table 4. Samples for DGEBA/diamine networks

Sample	Molar ratio* of [E] : [H] _{D230} : [H] _{D2000 (or D400)}
A: DGEBA + 100%D230	1 : 1 : 0
B: DGEBA + 99%D230 + 1%D2000	1 : 0.99 : 0.01
C: DGEBA + 98%D230 + 2%D2000	1 : 0.98 : 0.02
D: DGEBA + 95%D230 + 5%D2000	1 : 0.95 : 0.05
E: DGEBA + 98%D230 + 2%D400	1 : 0.98 : 0.02
F: DGEBA + 95%D230 + 5%D400	1 : 0.95 : 0.05
G: DGEBA + 90%D230 + 10%D400	1 : 0.90 : 0.10

*[E]: Epoxide monomer

[H]_{D230}: Hydrogen contributed by D230

[H]_{D400}: Hydrogen contributed by D400

[H]_{D2000}: Hydrogen contributed by D2000

3.2.2. Sample Characterization

The TA Instruments Differential Scanning Calorimeter (Modulated DSC) 2920 applies an enthalpy-change method to determine the difference in energy flow into a material as a function of temperature. These measurements are all taken in relationship to a reference material under a controlled temperature program. The glass transition temperature is where an amorphous solid becomes rubbery. The glass transition is

accompanied by a change in heat flow of the sample and therefore will be indicated on the DSC curve.

The glass transition temperature, T_g , and the changes in heat capacity ΔC_p at T_g for the testing samples were determined by the MDSC. The temperature scale was calibrated with the melting transition of indium. Temperature scans were performed at $5^\circ \text{C} / \text{min}$ with modulated $\pm 1^\circ \text{C}$ every 60 seconds and was operated over a temperature ranging from -60°C to $+120^\circ \text{C}$. Tests were performed on 10 to 20 mg samples. The heating scans were performed immediately after cooling samples which had been held at 120°C for 30 min to erase the thermal history. The T_g was taken by the inflection point, the point on the curve with the steepest slope, which is considered the midpoint of the step transition from glassy to the liquid state.

3.2.3 Physical Aging Experiments

The aging behavior was probed using the uniaxial extension under creep compliance and stress relaxation conditions. The mechanical tests were performed using a computer-controlled servo-hydraulic testing machine (Instron model 1321) equipped with an oven for temperature control. Measurements of the temperature between the top and bottom of the samples showed that the gradient was less than 0.6°C . Oven stability was better than $\pm 0.3^\circ \text{C}$ during each experiment. The dumbbell-shaped specimens were first annealed at 102°C (20°C above T_g of DGEBA/D230 determined by the D. S. C.) for 30 min to remove all previous aging, and then quickly placed in the testing machine at the testing temperature ($T_g - T = 15, 8, \text{ and } 5^\circ \text{C}$) where the glass began to age.

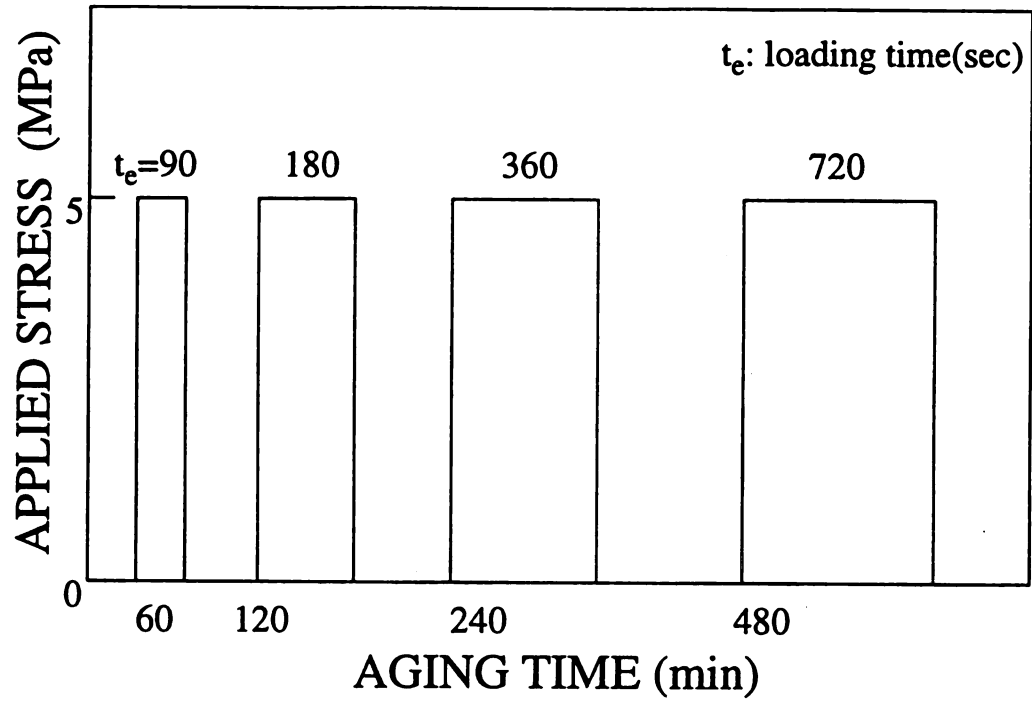


Figure 21. Schematic of stress history where all probes are of equal magnitude

Succ

with

defi

cree

MP

spe

rele

leng

was

stre

rela

Inst

app

def

us:

σ(t

3.2

(K

Successive deformations were applied at aging times, t_e , which approximately doubled with each test, i.e. $t_e = 60$ min, 120 min, 240 min etc (see Figure 21). At each interval of deformation, the ratio of the deformation duration time, t_i , to aging time was 0.05. In the creep compliance tests, the engineering stress applied to the samples were 1, 2.5, and 5 MPa respectively. The strain was measured with an Instron extensometer attached to the specimen. Because the specimens did not return to zero deformation as the applied stress released, the residual strain was subtracted from the total strain and the specimen gauge length was corrected for each loading interval of the aging test. The creep compliance was then calculated at $\epsilon(t) / \sigma$, where $\epsilon(t)$ is the corrected strain and σ is the engineering stress, determined from the original cross-sectional area of the specimen. In the stress relaxation tests, the applied strain, ϵ , in these tests was 0.1% and was measured with an Instron extensometer. Successive deformations were applied at aging time, t_e , which approximately doubled with each test. At each interval of deformation, the ratio of deformation duration time, t_i , to aging time was 0.05. The stress, $\sigma(t)$, was measured using a 2000lb (900 kg) capacity load cell. Thus the stress relaxation modulus was $E(t) = \sigma(t) / \epsilon$.

3.2.4. Data Analysis Method

The creep compliance curve was analysed using Kohlrausch-Williams-Watts (KWW) type function [28, 29]:

$$D(t) = D_0 \{ 1 + \exp [-(t/\tau)^\beta] \} \quad (2)$$

v

e

v

a

[

w

sh

su

ter

Th

wh

val

Th

wh

its

rate.

where $2D_0$ is the zero-time compliance, τ is a characteristic retardation time and the exponent β characterize the shape parameter for the creep curve and the width of the viscoelastic spectrum. To perform the superposition and a master curve, the value of D_0 and β at various aging time and temperature must be same.

The stress relaxation curve at a given aging time was curve fitted with the KWW [28, 29] stretched exponential function:

$$E(t) = E_0 \exp[-(t/\tau)^\beta] \quad (3)$$

where E_0 is the modulus at $t = 0$, τ is a characteristic relaxation time and β describes the shape of the relaxation curve and the width of the viscoelastic spectrum. To perform the superposition and a master curve, the value of E_0 and β at the various aging time and temperature must be same.

The aging time shift factor a_{t_e} is defined in terms of the KWW [28, 29] function as:

$$a_{t_e} = \tau(t_e) / \tau(t_{er}) \quad (4)$$

where $\tau(t_e)$ is the value of τ in equation (2, 3) at the aging time t_e and $\tau(t_{er})$ is its value at the reference aging time.

The temperature shift factor a_T is defined in terms of the KWW [28, 29] function as:

$$a_T = \tau(t_e) / \tau(t_e) \quad (5)$$

where $\tau(t_e)$ is the value of τ in the equation (2, 3) at the aging temperature and $\tau(t_e)$ is its value at the reference temperature.

The aging process is conveniently characterized by the double-logarithmic shift rate, μ , defined as (4):

$$\mu = d \log a_{t_e} / d \log t_e \quad (6)$$

3.3 Results and Discussion

3.3.1 DSC Results

Table 5. DSC results for the DGEBA/diamine networks

Sample	T _g (° C)	ΔC _p (J/g° C)	Glass transition zone (° C)
DGEBA+100%D230	82.89	0.1208	10.30
DGEBA+99%D230+1%D2000	78.65	0.1325	13.45
DGEBA+98%D230+2%D2000	74.78	0.1343	13.83
DGEBA+95%D230+5%D2000	65.35	0.1370	19.23
DGEBA+98%D230+2%D400	82.50	0.1349	11.25
DGEBA+95%D230+5%D400	78.06	0.1360	11.52
DGEBA+90%D230+10%D400	75.33	0.1364	11.56

In Table 5, the value of T_g and the change in heat capacity ΔC_p at T_g as determined by D. S. C. for all the epoxy networks were listed. One can see from the table that when D400 or D2000 is added to D230, T_g decreased, the ΔC_p at T_g increased by more than 10%. The glass transition zone, changed from rubber to glassy state, is broadened by adding D2000, but it doesn't change very much by adding D400. Since D2000 is long chain diamine (compared to D230 and D400), when mixing D2000, the distance between the crosslink point in the epoxy network is no longer same. The length between crosslink junction networks are no longer homogeneous and the ΔC_p increase during glass transition with decreases T_g. From Figures 4-10., one can see that there is no phase separation has occurred when mixing small amount of D400 and D2000, since there is

only one glass transition temperature for each specimen. It is important evidence that no gross segregation occurs between these two diamine chains, otherwise one would detect two distinct transitions. So the DGEBA/diamine networks are compatible and the samples containing two diamines with a regularly alternating long and short diamine chains are single-phase materials.

3.3.2 Creep Test Results

3.3.2.1 Boltzmann Superposition

The use of the Boltzmann superposition principle can be applied in the creep compliance tests for all epoxy networks. In creep compliance tests, a stress of σ_0 is applied at $t = 0$ and take off at $t = t_i$ (duration time). The strain due to loading, e_1 , is given by $e_1 = \sigma_0 D(t)$ and that due to unloading is similarly $e_2 = -\sigma_0 D(t - t_i)$. The total strain after time t ($> t_i$), $e(t)$ is given by $e(t) = \sigma_0 D(t) - \sigma_0 D(t - t_i)$. In this region $e(t)$ is decreasing and this process is known as recovery. If the recovered strain $e_3(t - t_i)$ is defined as the difference between the strain that would have occurred if the initial stress had been maintained and the actual strain then $e_3(t - t_i) = \sigma_0 D(t - t_i)$, which is identical to the creep strain expected for a stress of $+\sigma_0$ applied after a time t_i . Therefore, if $e_1 = e_3(t - t_i)$ then the Boltzmann superposition applied and the test is in linear viscoelastic range. If not, it is in nonlinear viscoelastic range. In this creep compliance tests, the $e_1 \neq e_3(t - t_i)$ for all tests. It proved that these creep compliance tests are in nonlinear viscoelastic range. Figure 22. shows a example of these tests.

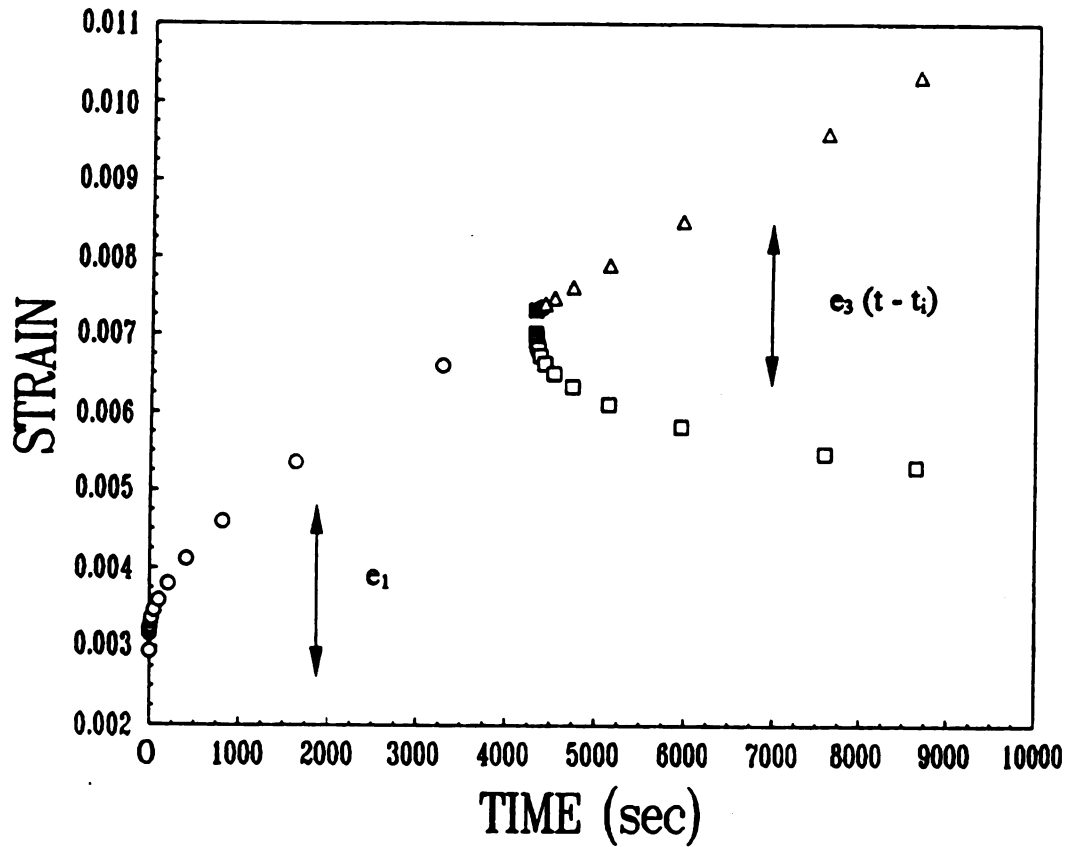


Figure 22. The response of DGEBA+100%D230 aged at 78.5° C for 24 hours to loading followed by unloading, illustrating the Boltzmann superposition principle. (O) loading; (□) unloading; (Δ) extroplated from loading curve

a
V
V
i
a
d
h
D
h
ex
The

3.3.2.2 Aging Results

In Figures 23-25, it was shown the double-logarithmic plots of creep compliance at the indicated aging times versus time for these epoxy networks at the 15° C below the D. S. C. measured Tg of each sample. The value of the applied stress in these experiments was 5 MPa. The KWW parameters for these data are tabulated in Table 6. It is evident that creep compliance during this time period of the experiment increases with sub Tg aging time, thus indicating an increase in the retardation times. This behavior occurs due to the decrease in molecular mobility as free volume decreases during physical aging. This reduced mobility causes molecular relaxations to become slower, thus shifting the relaxation spectrum to longer times as the physical aging process proceeds and the shorter time relaxations occur. Importantly, the values of D_0 and β do not vary with aging time for any given epoxy networks. However, the values of the width of the viscoelastic spectrum β and the retardation time τ decrease as D2000 increases. This indicates that the D2000 content have a greater resistance to creep. Although time - aging time superposition appears to be valid for these epoxy networks, time-crosslink density superposition is not in this temperature range for these epoxy networks.

The above creep compliance tests were performed after 16 hours physical aging. In Table 6 and Figure 26, it also showed that the aging time was 64 hours for DGEBA+95%D230+5%D2000, the sample was different with the aging time for 16 hours, but the results were similar, it proved that the experiments were repeatable. The experiment without intermittent stress was performed. The two curves were similar. Therefore, the successive loading will not affect the results in small strain range.

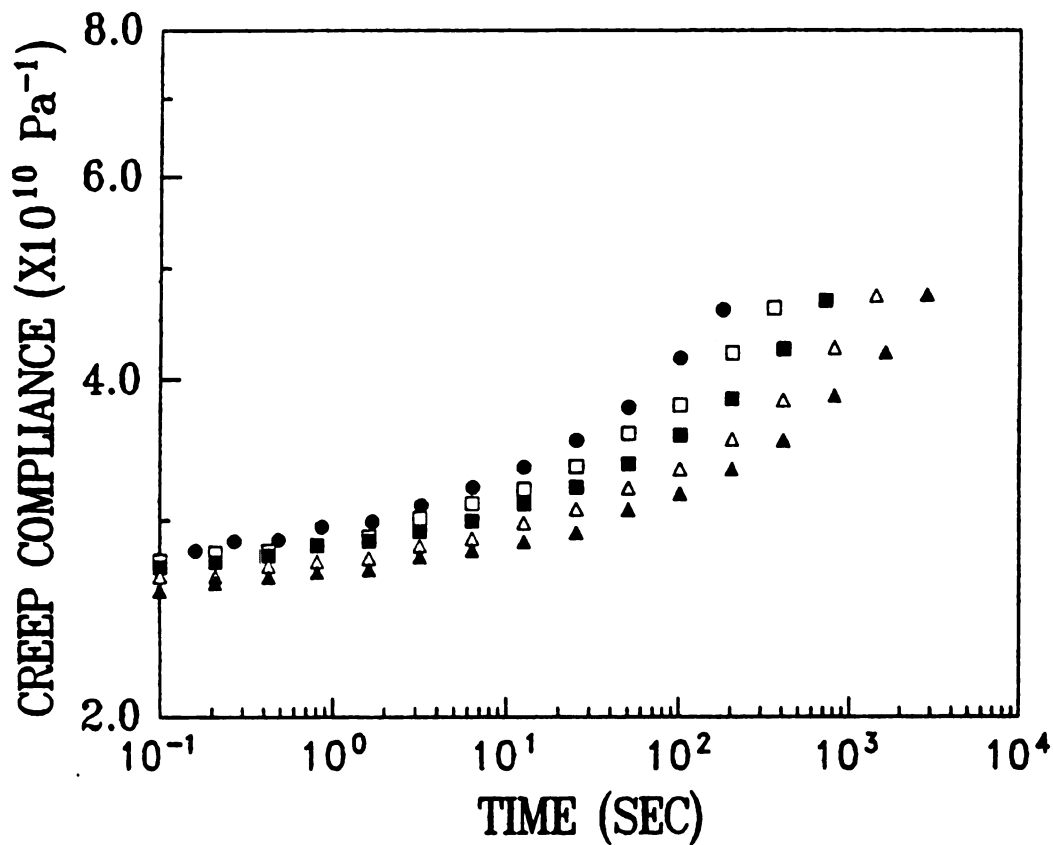


Figure 23. Creep compliance curves for DGEBA + 100%D230 quenched from 102° C (i.e. 20° C above T_g of DGEBA/D230) to 66.9° C and kept at $66.9 \pm 0.3^\circ$ C for a period of time. The applied engineering stress is 5 MPa; β is 0.2851 and D_0 is $1.3075 \times 10^{10} \text{ Pa}^{-1}$. The different curves were measured at various aging time indicated: (●) 60 min; (□) 120 min; (■) 240 min; (△) 480 min; (▲) 960 min

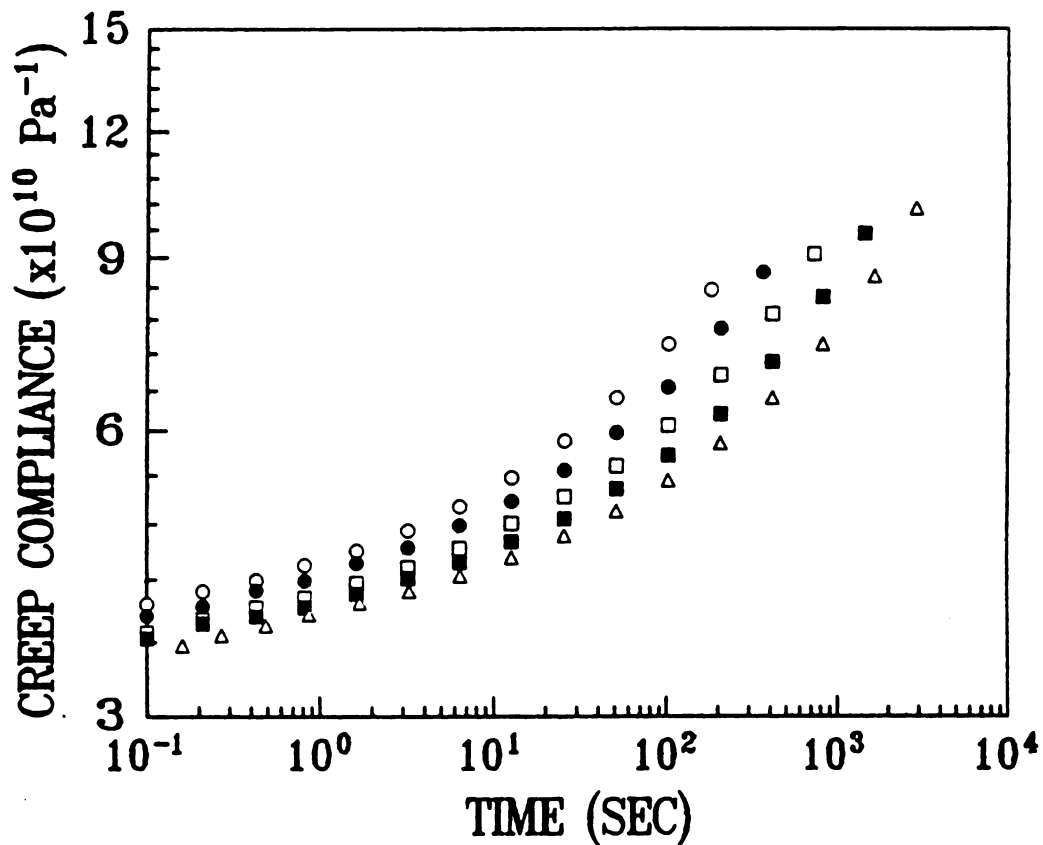


Figure 24. Creep compliance curves for DGEBA + 98%D230 + 2%D2000 quenched from 102° C (i.e. 20° C above T_g of DGEBA/D230) to 61.1° C and kept at 61.1 ± 0.3° C for a period of time. The applied engineering stress is 5 MPa; β is 0.2171 and D₀ is 1.6831 (x 10¹⁰ Pa⁻¹). The different curves were measured at various aging time indicated: (O) 60 min; (●) 120 min; (□) 240 min; (■) 480 min; (Δ) 960 min

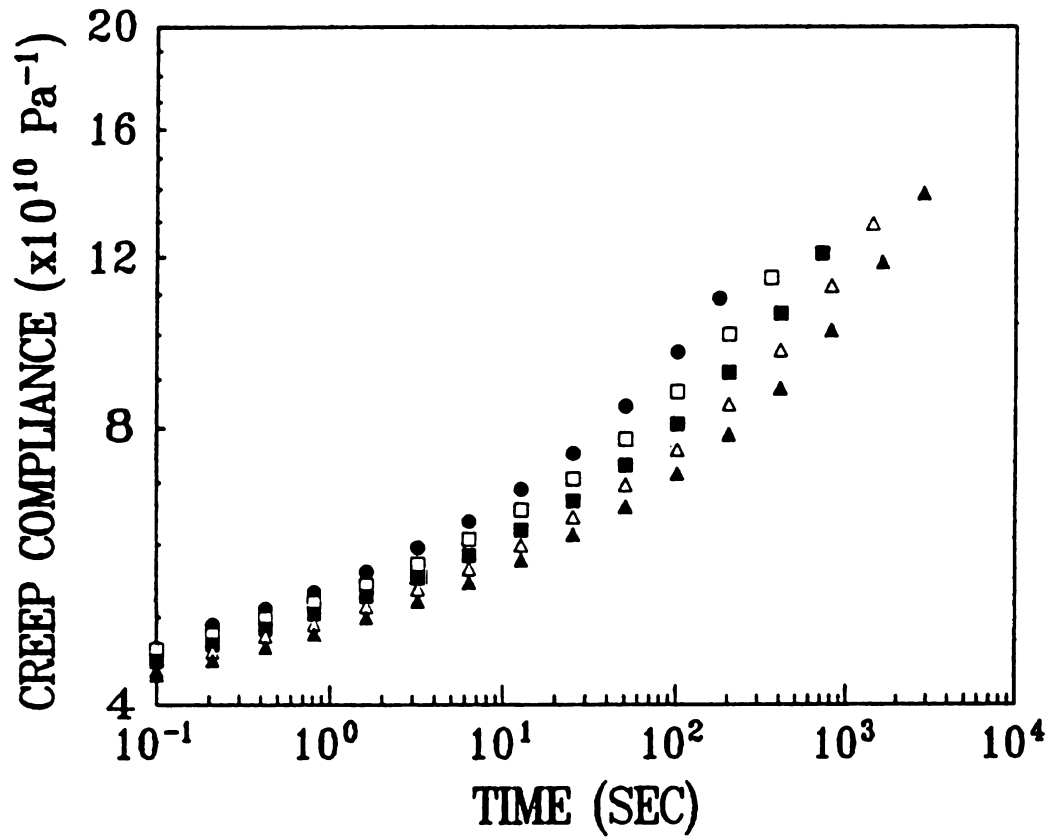


Figure 25. Creep compliance curves for DGEBA+95%D230 +5%D2000 quenched from 102° C (i.e. 20° C above T_g of DGEBA/D230) to 49.6° C and kept at 49.6 ± 0.3° C for a period of time. The applied engineering stress is 5 MPa; β is 0.1769 and D_0 is 1.8827 ($\times 10^{10}$ Pa⁻¹). The different curves were measured at various aging time indicated: (●) 60 min; (□) 120 min; (■) 240 min; (△) 480 min; (▲) 960 min

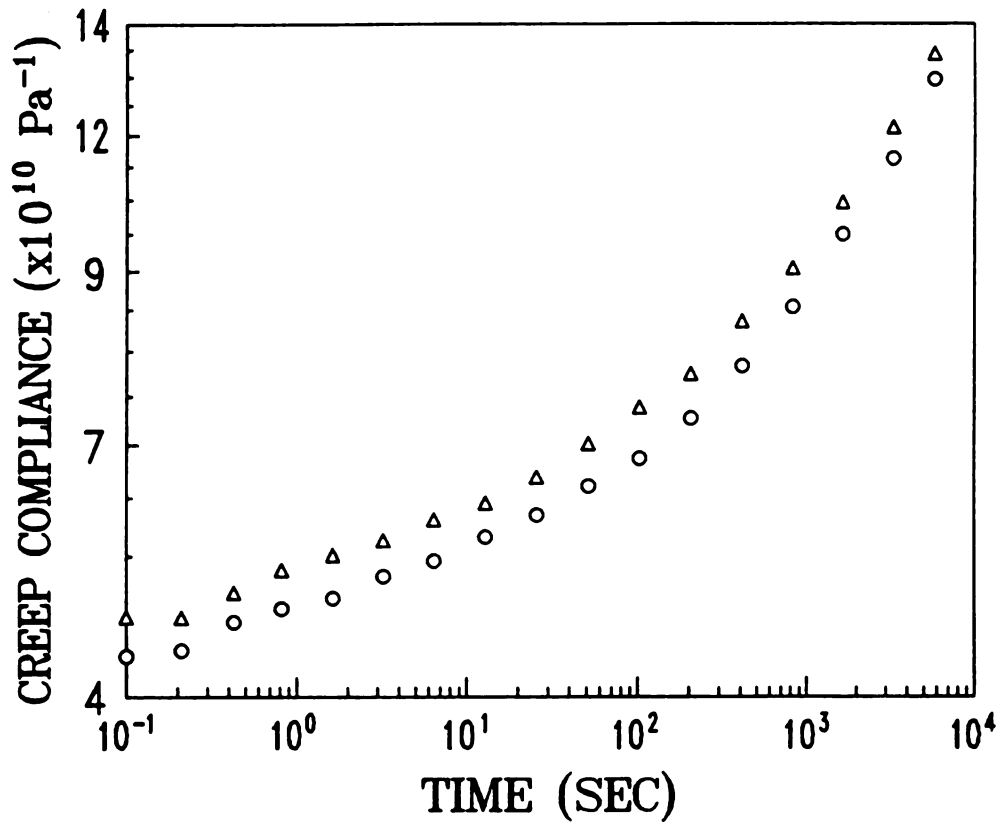


Figure 26. Creep compliance curves for DGEBA+95%D230+5%D2000 quenched from 102° C (i.e. 20° C above T_g of DGEBA/D230) to 49.5° C and kept at 49.5 ± 0.3° C for a period of time. The applied engineering stress is 5 MPa. The different curves were measured at different stress histories indicated: (O) without intermittent stress; (Δ) with intermittent stress

Table 6. KWW curve fitting parameters for Tg-15° C; σ is 5 MPa

Sample	t (min)	D_0 ($\times 10^{10}$ Pa ⁻¹)	τ (s)	β
DGEBA+100%D230 T* : 66.9° C	60	1.34	268.13	0.29
	120	1.31	479.64	0.28
	240	1.31	899.87	0.28
	480	1.29	1591.01	0.28
	960	1.27	2930.01	0.27
DGEBA+98%D230+2%D2000 T* : 61.1° C	60	1.74	51.35	0.22
	120	1.71	77.11	0.22
	240	1.66	110.68	0.21
	480	1.66	188.98	0.21
	960	1.62	263.52	0.20
DGEBA+95%D230+5%D2000 T* : 49.6° C	60	1.90	14.49	0.18
	120	1.90	25.66	0.17
	240	1.87	36.44	0.17
	480	1.86	52.72	0.17
	960	1.87	84.48	0.17
DGEBA+95%D230+5%D2000** T* : 49.5° C	60	2.13	18.83	0.18
	120	2.09	26.54	0.17
	240	2.08	37.22	0.17
	480	2.04	54.80	0.17
	960	2.04	83.06	0.17
	1920	2.02	123.31	0.16
	3840	2.00	199.26	0.16
DGEBA+95%D230+5%D2000***	3840	1.90	211.09	0.17
DGEBA+98%D230+2%D400 T* : 69.0° C	60	1.48	107.58	0.27
	120	1.47	240.55	0.28
	240	1.43	444.79	0.27
	480	1.41	815.11	0.27
	960	1.41	1512.51	0.27
DGEBA+90%D230+10%D400 T* : 60.3° C	60	1.49	332.16	0.26
	120	1.46	573.45	0.26
	240	1.45	1083.61	0.27
	480	1.43	1870.44	0.26
	960	1.41	3378.34	0.26

T* : aging temperature for each sample

** : different sample for longer aging time

*** : different sample without intermittent stress

In Figures 27-30, it was shown the double-logarithmic plots of creep compliance at indicated aging time versus time for these epoxy networks, but the aging temperature is at the 8° C below the D. S. C. measured T_g of each sample. The applied stress was 2.5 MPa. The KWW parameters for these datas are tabulated in Table 7. Again, it is observed that the values of D₀ and β do not vary with aging time for any given epoxy networks. The time-aging time superposition appear to be valid for these epoxy networks, but time-crosslink density superposition is not valid.

One also carried out experiment at the temperature closed to T_g (T_g - T = 5° C) and the applied stress is 1 MPa. The curves are plotted in Figures 31-33. The results of KWW analysis are tabulated in Table 8. It is observed that the values of D₀ and β do not vary with aging time for any given epoxy networks. In Figure 33, the creep curves are plotted at increasing aging time for sample of DGEBA+95%D230+5%D2000 network at 5° C below the D. S. C. measured T_g. It is apparent from this curve that after approximately 120 min of aging the creep curves no longer shift to longer time, i.e. aging has ceased and equilibrium has been reached. It is indicated that the time dependent creep compliance rises faster with a short aging time (i.e., has a higher creep rate). This is a direct consequence of the increased molecular mobility with short aging time. Again, time-aging time superposition was found to be valid, but time-crosslink density superposition was not.

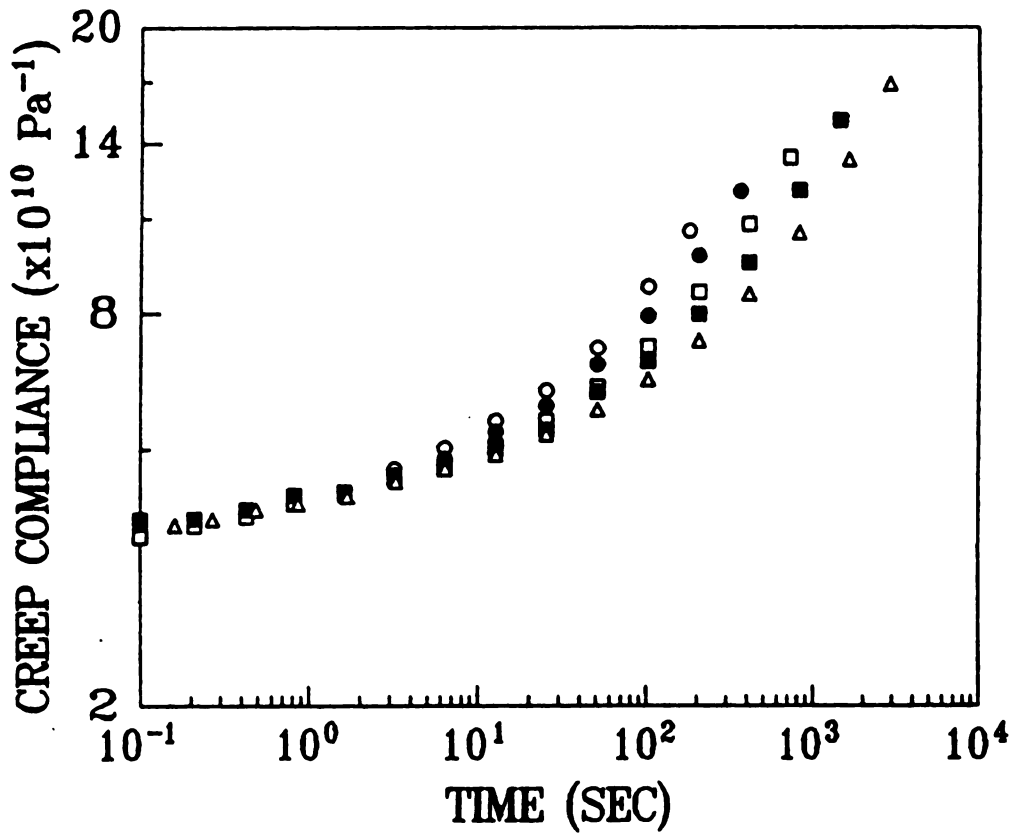


Figure 27. Creep compliance curves for DGEBA + 100%D230 quenched from 102° C (i.e. 20° C above T_g of DGEBA/D230) to 75.2° C and kept at $75.2 \pm 0.3^\circ$ C for a period of time. The applied engineering stress is 2.5 MPa; β is 0.2508 and D_0 is $1.6986 (\times 10^{10} \text{ Pa}^{-1})$. The different curves were measured at various aging time indicated: (O) 60 min; (●) 120 min; (□) 240 min; (■) 480 min; (Δ) 960 min

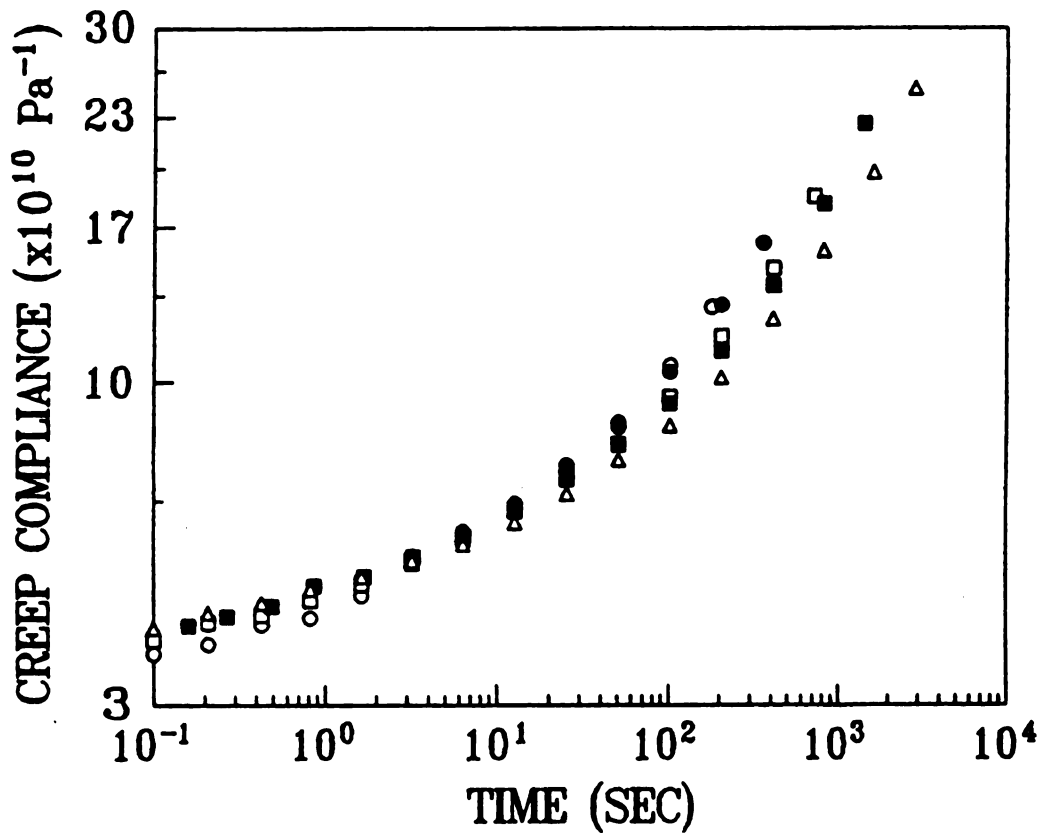


Figure 28. Creep compliance curves for DGEBA+98%D230 +2%D2000 quenched from 102° C (i.e. 20° C above T_g of DGEBA/D230) to 66.6° C and kept at 66.6 ± 0.3° C for a period of time. The applied engineering stress is 2.5 MPa; β is 0.1968 and D_0 is 1.5465 ($\times 10^{10}$ Pa⁻¹). The different curves were measured at various aging time indicated: (O) 60 min; (●) 120 min; (□) 240 min; (■) 480 min; (Δ) 960 min

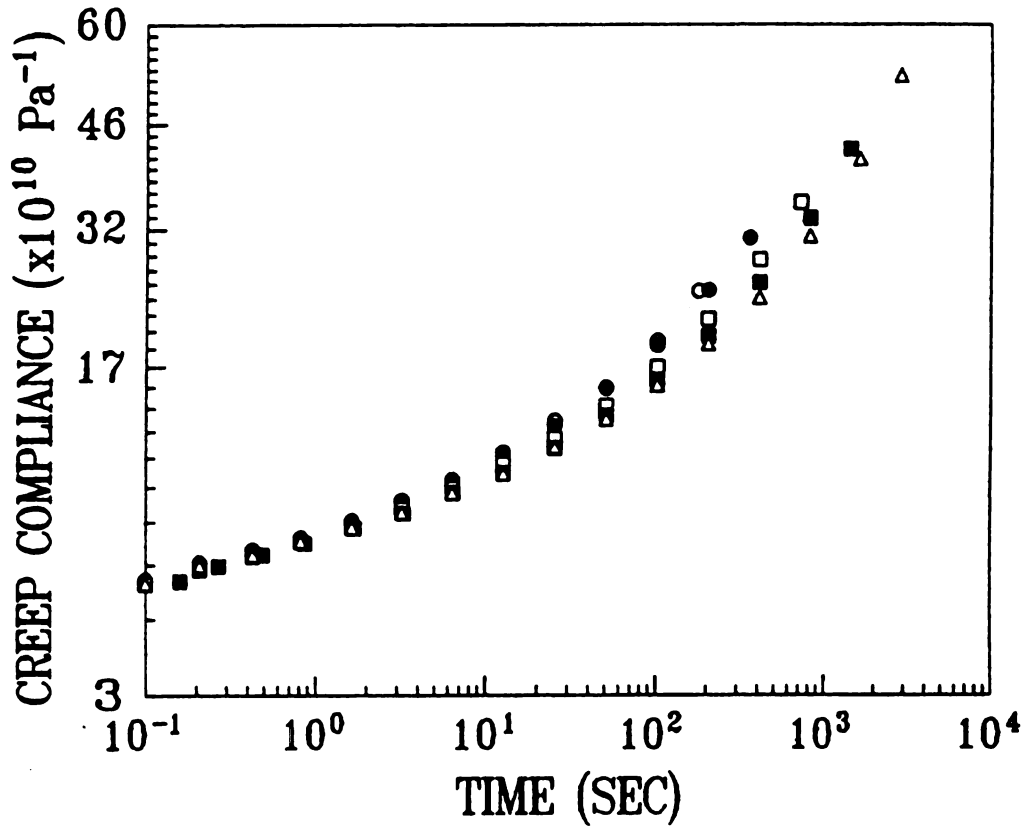


Figure 29. Creep compliance curves for DGEBA+95%D230+ 5%D2000 quenched from 102° C (i.e. 20° C above T_g of DGEBA/D230) to 58.0° C and kept at 58.0 ± 0.3° C for a period of time. The applied engineering stress is 2.5 MPa; β is 0.1583 and D₀ is 1.8983 (x 10¹⁰ Pa⁻¹). The different curves were measured at various aging time indicated: (O) 60 min; (●) 120 min; (□) 240 min; (■) 480 min; (Δ) 960 min

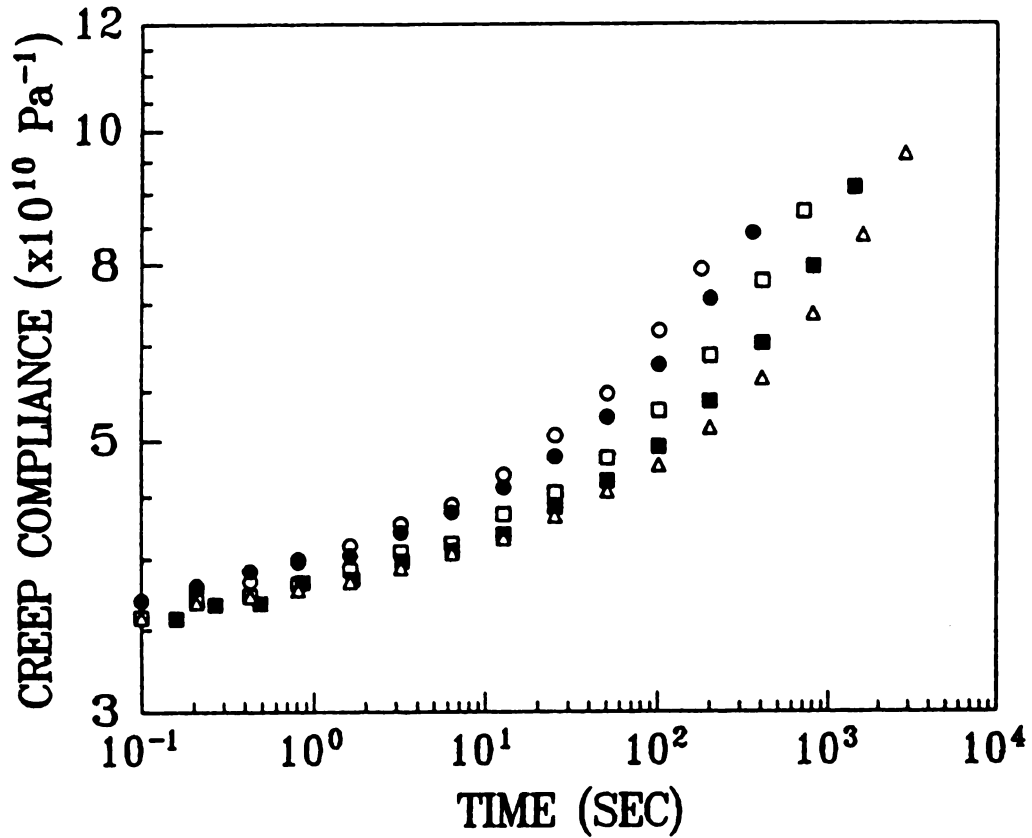


Figure 30. Creep compliance curves for DGEBA+90%D230+10%D400 quenched from 102° C (i.e. 20° C above T_g of DGEBA/D230) to 66.7° C and kept at 66.7 ± 0.3° C for a period of time. The applied engineering stress is 2.5 MPa; β is 0.2636 and D_0 is 1.7561 ($\times 10^{10} \text{ Pa}^{-1}$). The different curves were measured at various aging time indicated: (O) 60 min; (●) 120 min; (□) 240 min; (■) 480 min; (Δ) 960 min

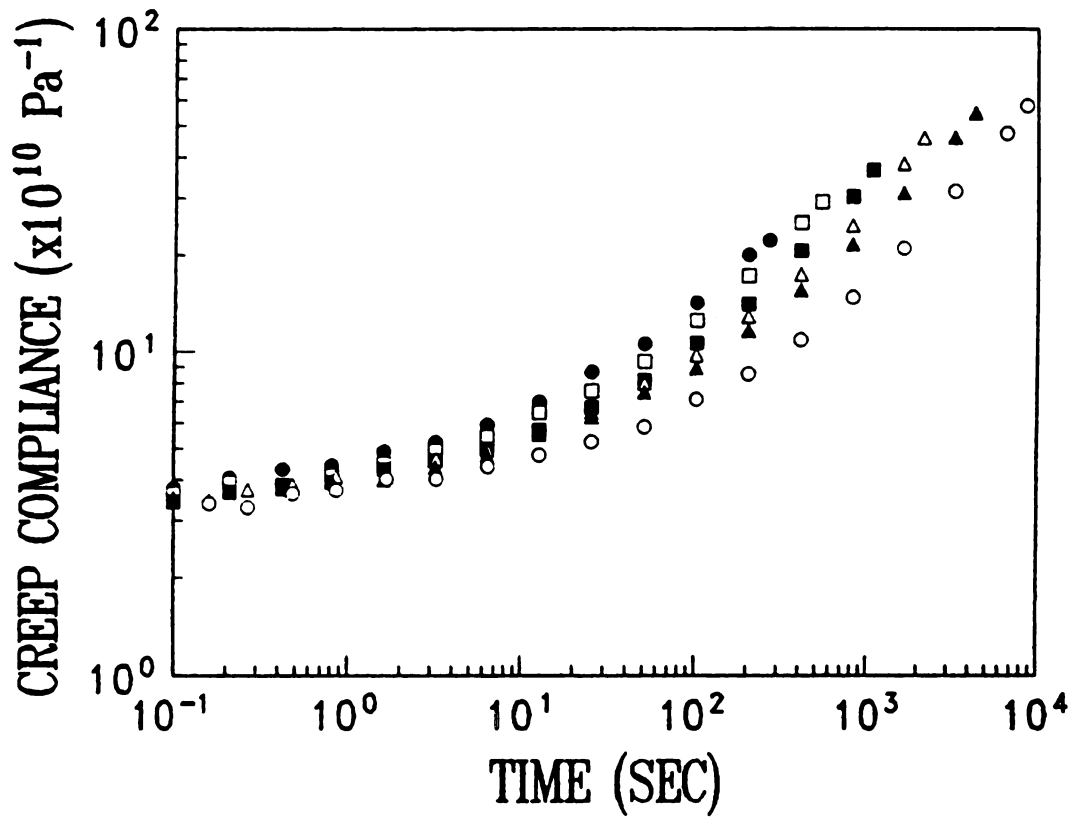


Figure 31. Creep compliance curves for DGEBA + 100%D230 quenched from 102° C (i.e. 20° C above T_g of DGEBA/D230) to 78.5° C and kept at 78.5 ± 0.3° C for a period of time. The applied engineering stress is 1 MPa; β is 0.2099 and D_0 is 1.3472 ($\times 10^{10} \text{ Pa}^{-1}$). The different curves were measured at various aging time indicated: (●) 90 min; (□) 180 min; (■) 360 min; (Δ) 720 min; (▲) 1440 min; (○) 2880 min

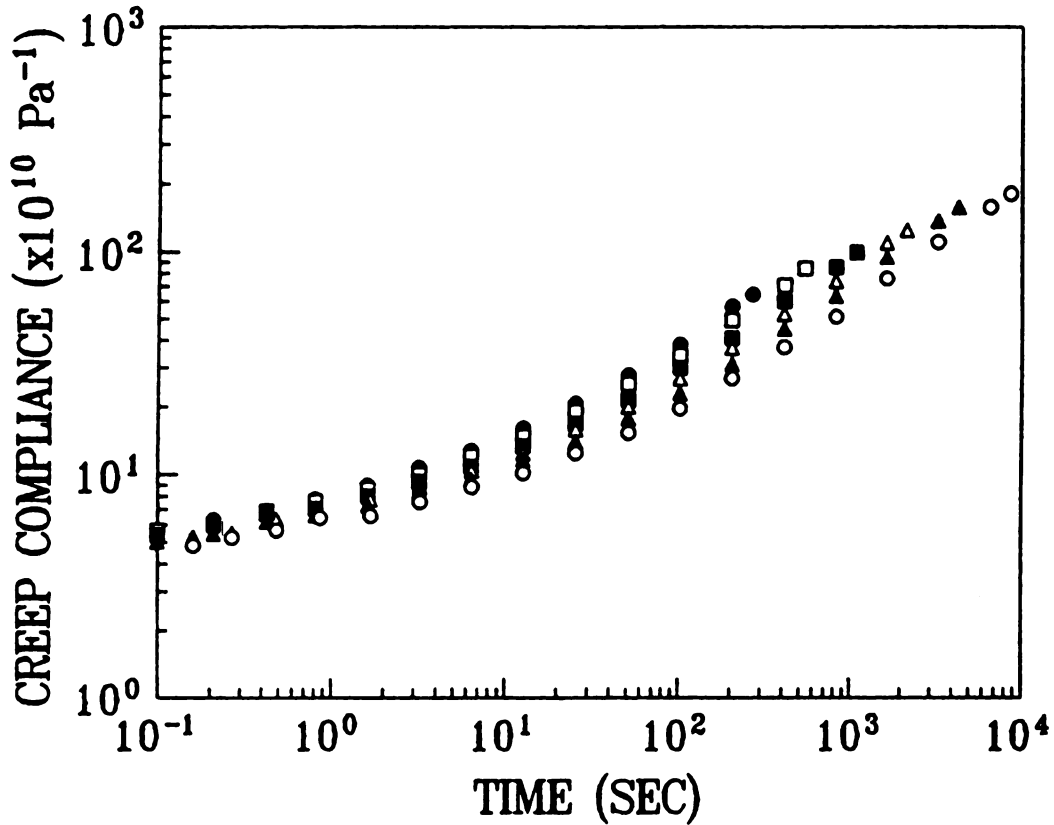


Figure 32. Creep compliance curves for DGEBA+98%D230+2%D2000 quenched from 102° C (i.e. 20° C above T_g of DGEBA/D230) to 71.3° C and kept at 71.3 ± 0.3° C for a period of time. The applied engineering stress is 1 MPa; β is 0.1636 and D_0 is 1.6736 ($\times 10^{10}$ Pa⁻¹). The different curves were measured at various aging time indicated: (●) 90 min; (□) 180 min; (■) 360 min; (Δ) 720 min; (▲) 1440 min; (○) 2880 min

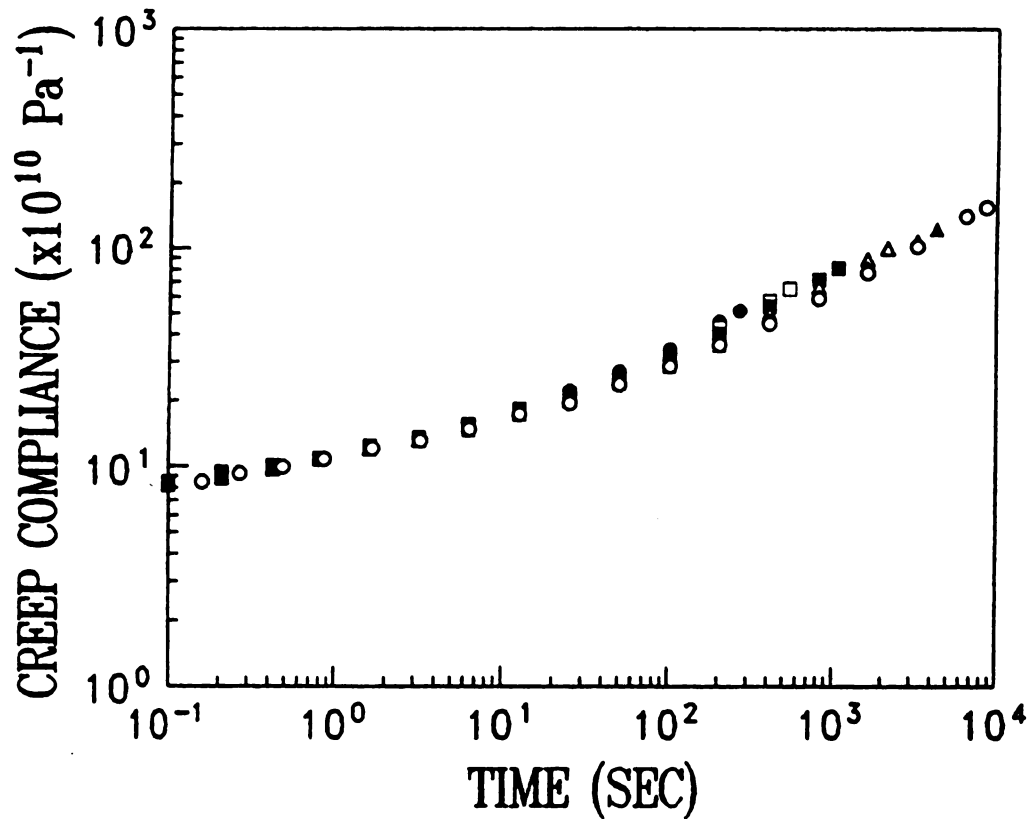


Figure 33. Creep compliance curves for DGEBA+95%D230+5%D2000 quenched from 102° C (i.e. 20° C above T_g of DGEBA/D230) to 60.8° C and kept at 60.8 ± 0.3° C for a period of time. The applied engineering stress is 1 MPa; β is 0.1388 and D_0 is 2.2504 (x 10¹⁰ Pa⁻¹). The different curves were measured at various aging time indicated: (●) 90 min; (□) 180 min; (■) 360 min; (Δ) 720 min; (▲) 1440 min; (O) 2880 min

Table 7. KWW curve fitting parameters for $T_g - 8^\circ \text{C}$; σ is 2.5MPa

Sample	t (min)	D_0 ($\times 10^{10} \text{ Pa}^{-1}$)	τ (s)	β
DGEBA+100%D230 $T^* : 75.2^\circ \text{C}$	60	1.67	26.43	0.26
	120	1.66	34.19	0.25
	240	1.67	52.19	0.25
	480	1.75	79.43	0.24
	960	1.72	105.17	0.23
DGEBA+98%D230+2%D2000 $T^* : 66.6^\circ \text{C}$	60	1.40	4.69	0.20
	120	1.53	6.77	0.20
	240	1.53	9.34	0.19
	480	1.62	12.14	0.19
	960	1.63	15.09	0.18
DGEBA+95%D230+5%D2000 $T^* : 58.0^\circ \text{C}$	60	1.81	0.56	0.15
	120	1.93	0.89	0.16
	240	1.89	0.94	0.15
	480	1.89	1.12	0.15
	960	1.94	1.24	0.15
DGEBA+90%D230+10%D400 $T^* : 67.8^\circ \text{C}$	60	1.73	93.42	0.25
	120	1.78	157.86	0.26
	240	1.73	243.82	0.26
	480	1.75	439.01	0.26
	960	1.76	698.38	0.26

T^* : aging temperature for each sample

Table 8. KWW curve fitting parameters for $T_g - 5^\circ \text{C}$; σ is 1 MPa

Sample	t (min)	D_0 ($\times 10^{10} \text{ Pa}^{-1}$)	τ (s)	β
DGEBA+100%D230 T* : 78.5° C	45	1.46	1.87	0.21
	90	1.39	2.56	0.21
	180	1.34	3.35	0.21
	360	1.26	3.94	0.21
	720	1.27	4.31	0.20
	1440	1.34	5.08	0.19
DGEBA+98%D230+2%D2000 T* : 71.3° C	45	1.62	0.09	0.17
	90	1.61	0.12	0.16
	180	1.64	0.14	0.16
	360	1.66	0.16	0.16
	720	1.74	0.18	0.15
	1440	1.75	0.19	0.15
DGEBA+95%D230+5%D2000 T* : 60.8° C	45	2.02	0.08	0.14
	90	2.16	0.10	0.14
	180	2.18	0.11	0.14
	360	2.32	0.11	0.13
	720	2.37	0.12	0.13
	1440	2.42	0.12	0.13
DGEBA+90%D230+10%D400 T* : 67.8° C	45	2.22	1.75	0.21
	90	2.15	3.79	0.21
	180	2.21	3.87	0.20
	360	2.32	5.25	0.21
	720	2.15	6.18	0.19
	1440	2.28	8.61	0.19

T* : aging temperature for each sample

The time-temperature superposition principle was also investigated. Figures 34-35 depict a series of creep compliance curve at a constant aging time (60 min) as a function of temperature below T_g . A master curve can be obtained by simple horizontal shifting of the curves along the time axis, the arrow points to the shifting direction. The temperature shift factor, a_T , can be obtained from equation 5.

In Figures 36-38, show the double logarithmic plot of a_{te} versus t_e at different values of $T_g - T = 15, 8$ and 5°C for these epoxy networks. There are two features of interest in these figures. First, at each temperature range under the same applied stress, the value of the shift rate μ decreases as the amount of D2000 increases. Secondly, at the temperature approximately 5°C below T_g , these epoxy networks were able to age into structural equilibrium, i.e. the value of a_{te} become independent of aging time, where the shift rate μ (the slope of the plot) changes from a value near unity to virtually zero. Again this corresponds to the point where aging has arrested and equilibrium has been attained. This transition from aging to non - aging behavior is quite abrupt.

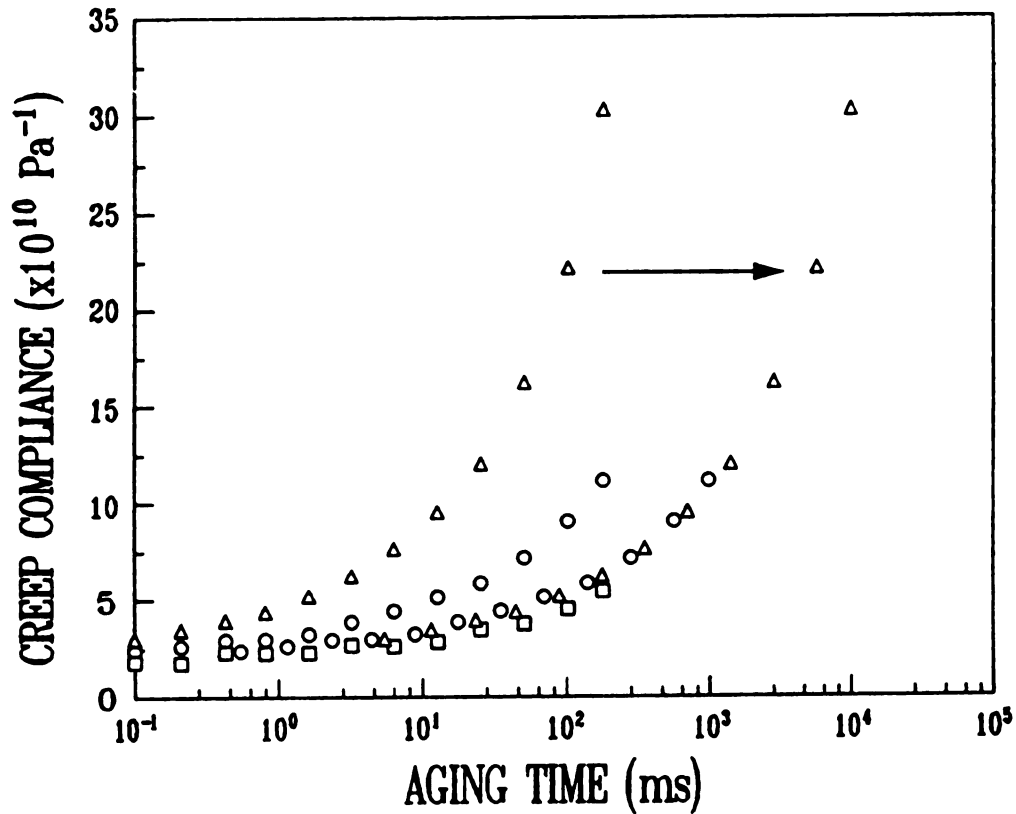


Figure 34. Creep compliance curves for DGEBA + 98%D230 + 2%D2000 aging at variant temperature for 60min. The applied engineering stress is 1 MPa. The curvatures of these curves were same, the master curves resulting from a superposition by time shift along the axis, so the time - temperature superposition were applied. The temperatures ($^{\circ}$ C): (Δ) 69.9; (O) 65.9; (\square) 60.7 (the shifting reference temperature)

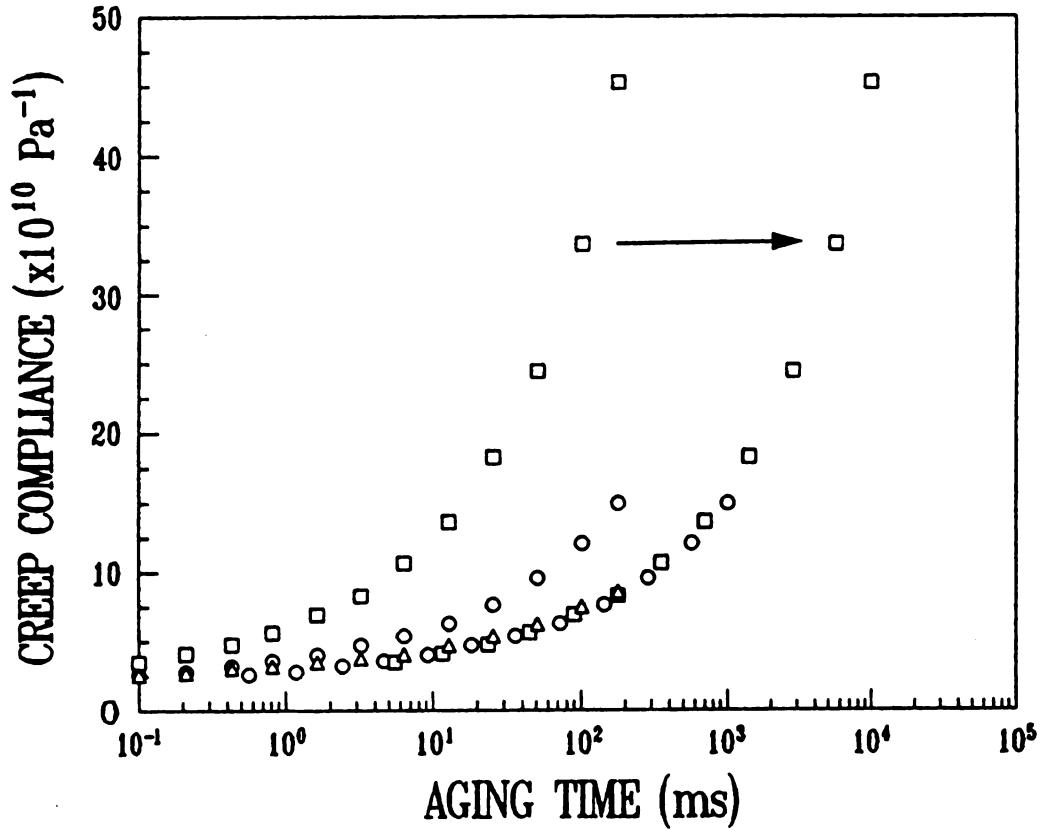


Figure 35. Creep compliance curves for DGEBA + 95%D230 + 5%D2000 aging at variant temperature for 60 min. The applied engineering stress is 1 MPa. The curvatures of these curves were same, the master curves resulting from a superposition by time shift along the axis, so the time-temperature superposition were applied. The temperatures ($^{\circ}$ C): (\square) 59.8; (\circ) 55.1; (Δ) 50.4 (the shifting reference temperature)

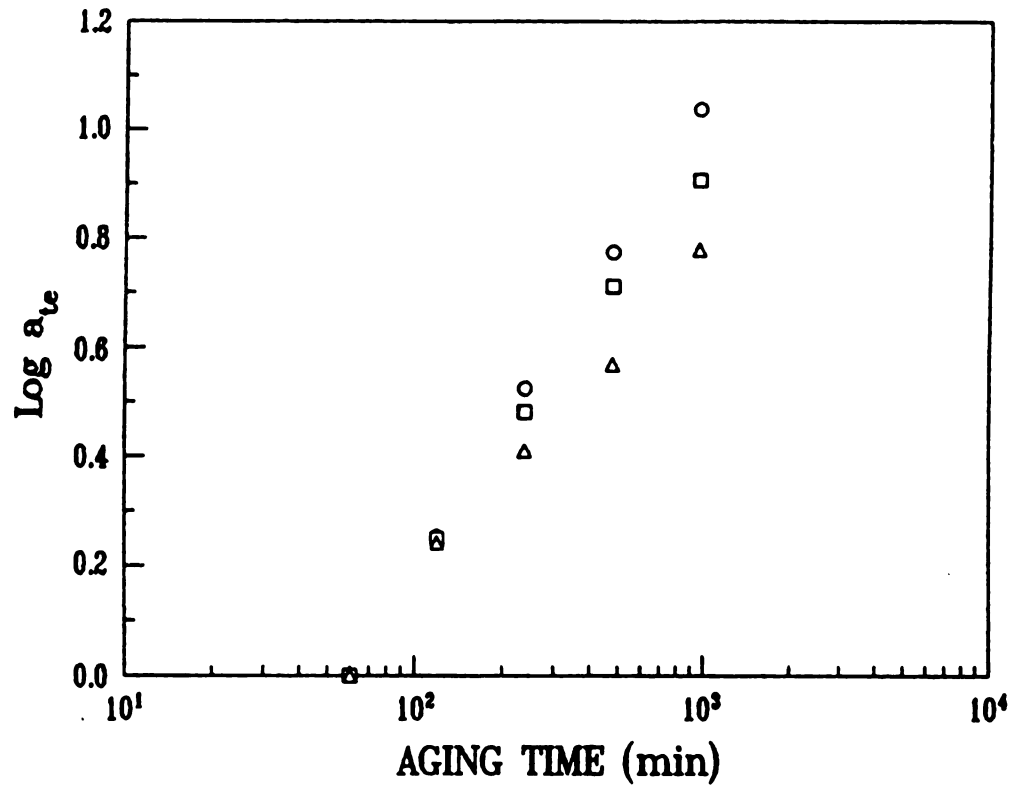


Figure 36. Double logarithmic plot of aging time shift factor a_{te} versus aging time for all the sample at $T_g - 15^\circ \text{C}$, the reference aging time was chosen as 60 min for each sample. The applied stress is 5 MPa. (O) DGEBA + 100%D230; (□) DGEBA + 98%D230 + 2%D2000; (Δ) DGEBA + 95%D230 + 5%D2000

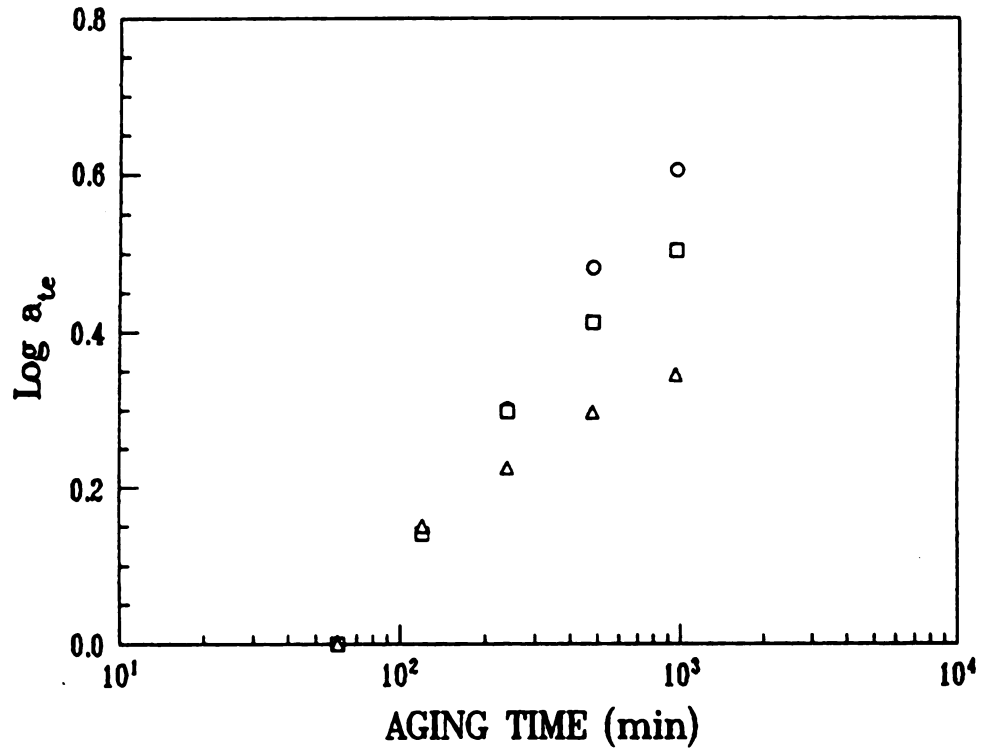


Figure 37. Double logarithmic plot of aging time shift factor a_{te} versus aging time for all the sample at $T_g - 8^\circ \text{C}$, the reference aging time was chosen as 60 min for each sample. The applied stress is 2.5 MPa. (O) DGEBA + 100%D230; (□) DGEBA + 98%D230 + 2%D2000; (Δ) DGEBA + 95%D230 + 5%D2000

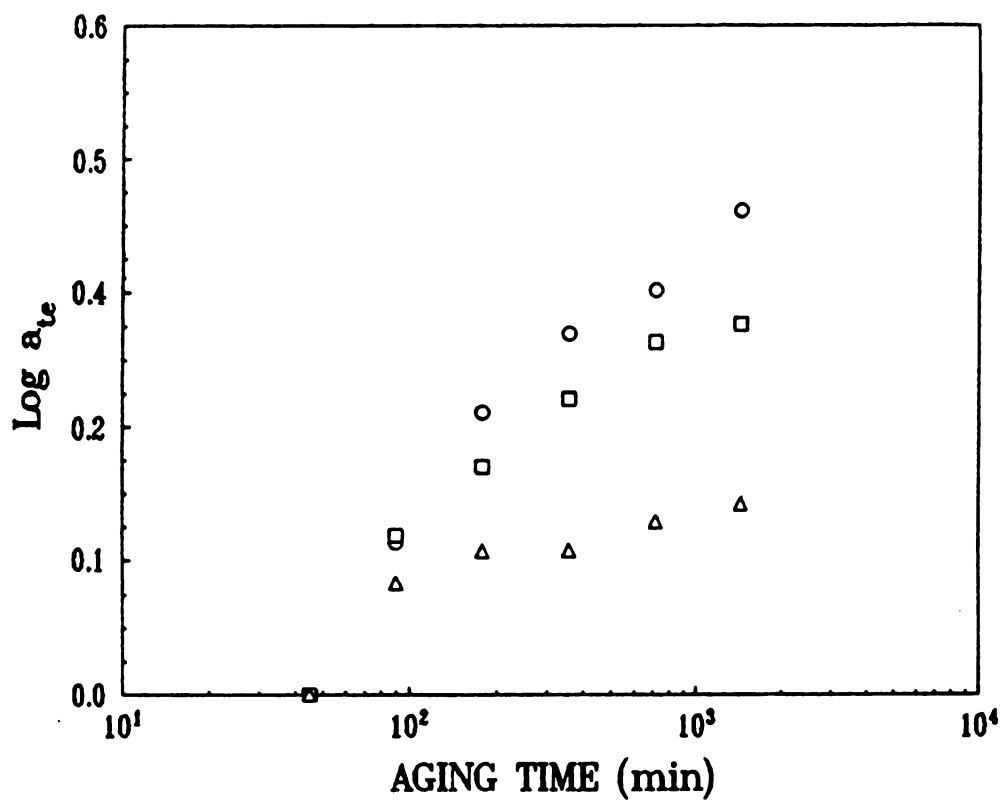


Figure 38. Double logarithmic plot of aging time shift factor a_{te} versus aging time for all the sample at $T_g - 5^\circ \text{C}$, the reference aging time was chosen as 60 min for each sample. The applied stress is 1 MPa. (O) DGEBA + 100%D230; (□) DGEBA + 98%D230 + 2%D2000; (Δ) DGEBA + 95%D230 + 5%D2000

3.3.3 Stress Relaxation Results

3.3.3.1 Boltzmann Superposition

It is possible to analyse stress relaxation in a similar way as using the Boltzmann superposition principle in creep compliance tests. In this case it is necessary to define a stress relaxation modulus $E(t)$ which relates the time-dependent stress $\sigma(t)$ to the strain e through the relationship $\sigma(t) = E(t) e$. When a strain of e_0 is applied at time $t = 0$ and take off at $t = t_i$ (duration time). The stress due to applied strain, σ_1 , is given by $\sigma_1 = e_0 E(t)$ and that due to releasing strain is similarly $\sigma_2 = -e_0 E(t - t_i)$. The total stress after time t ($> t_i$), $\sigma(t)$ is given by $\sigma(t) = e_0 E(t) - e_0 E(t - t_i)$. In this region $\sigma(t)$ is increasing and this process is known as recovery. If the recovered stress $\sigma_3(t - t_i)$ is defined as the difference between the stress that would have occurred if the initial strain had been maintained and the actual stress then is identical to the stress expected for a strain of e_0 applied for a time t_i . Therefore, if $\sigma_1 = \sigma_3(t - t_i)$, then the Boltzmann superposition applied. The tests are in linear viscoelastic range. In this stress relaxation tests, all the experimental data obey this condition. Therefore, the stress relaxation tests are in linear viscoelastic range. In Figure 39. show a example of these tests.

3.3.3.2 Aging Results

Figures 40-43 depict the family of stress relaxation isotherms for the relaxation modulus, $E(t)$, at $T_g - T = 15^\circ \text{C}$, obtained for these epoxy networks at various aging times, as indicated. The KWW parameters for these data are tabulated in Table 9. The

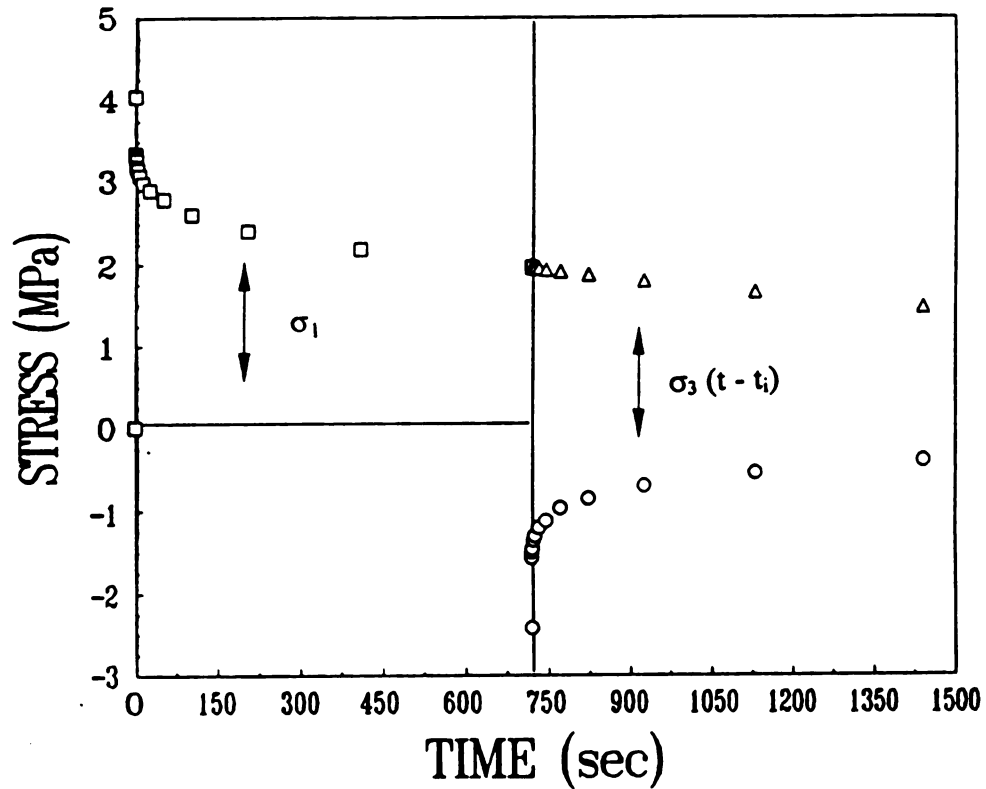


Figure 39. The response of DGEBA + 98%D230 + 2%D2000 aged at 60.8° C for 4 hours to loading followed unloading, illustrating the Boltzmann superposition principle. (□) loading; (Δ) unloading; (O) extropolated from loading curve

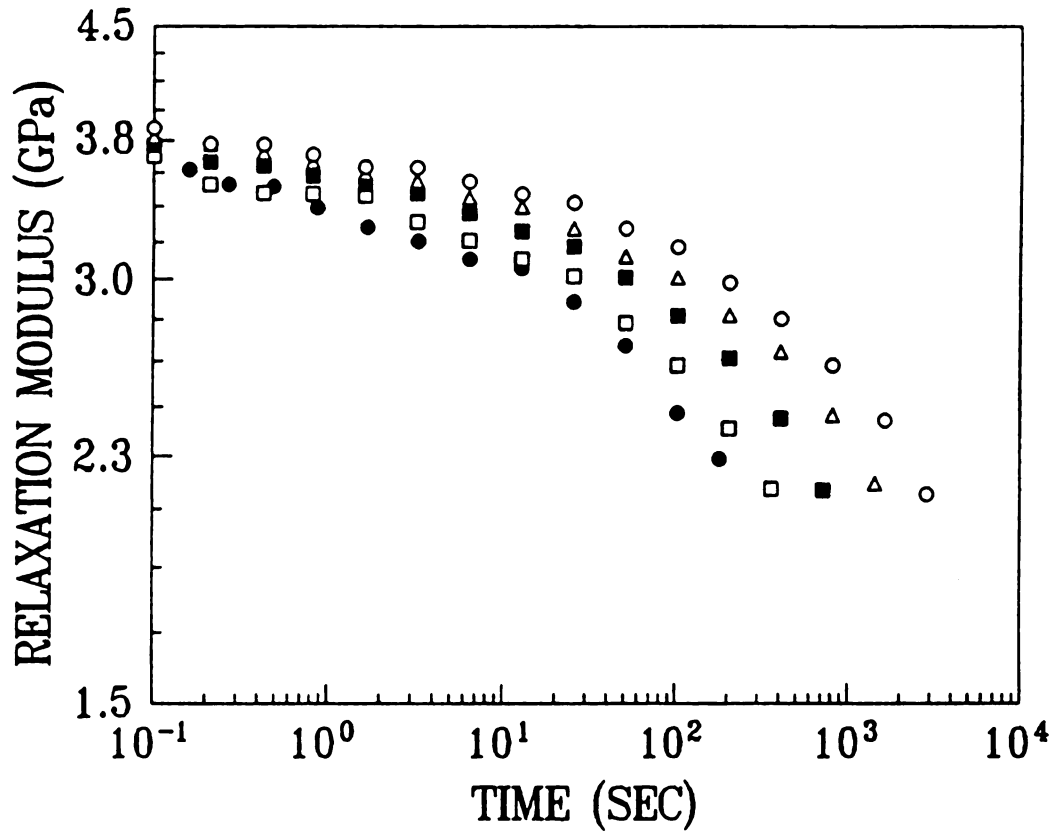


Figure 40. Stress relaxation curves for DGEBA + 100%D230 quenched from 102° C (i.e. 20° C above T_g of DGEBA/D230) to 67.9° C and kept at 67.9 ± 0.3° C for a period of time. The applied strain is 0.1%. The different curves were measured at various aging time indicated: (●) 60 min; (□) 120 min; (■) 240 min; (Δ) 480 min; (○) 960 min

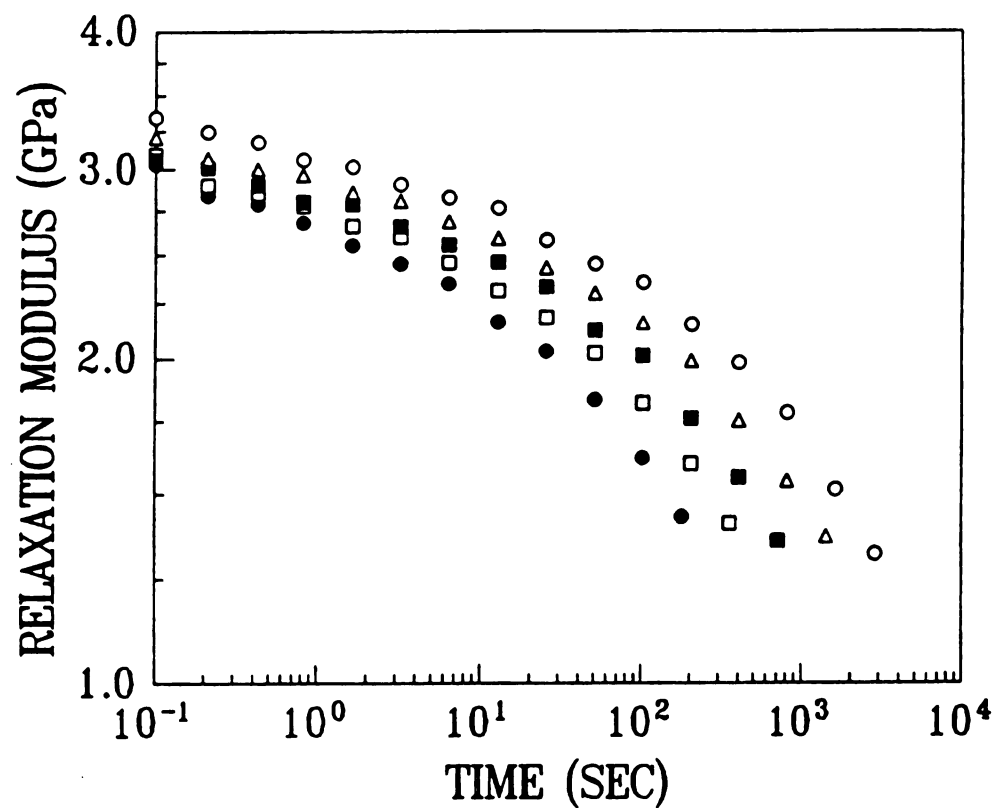


Figure 41. Stress relaxation curves for DGEBA + 98%D230 + 2%D2000 quenched from 102° C (i.e. 20° C above T_g of DGEBA/D230) to 60.8° C and kept at 60.8 ± 0.3° C for a period of time. The applied strain is 0.1%. The different curves were measured at various aging time indicated: (●) 60 min; (□) 120 min; (■) 240 min; (Δ) 480 min; (○) 960 min

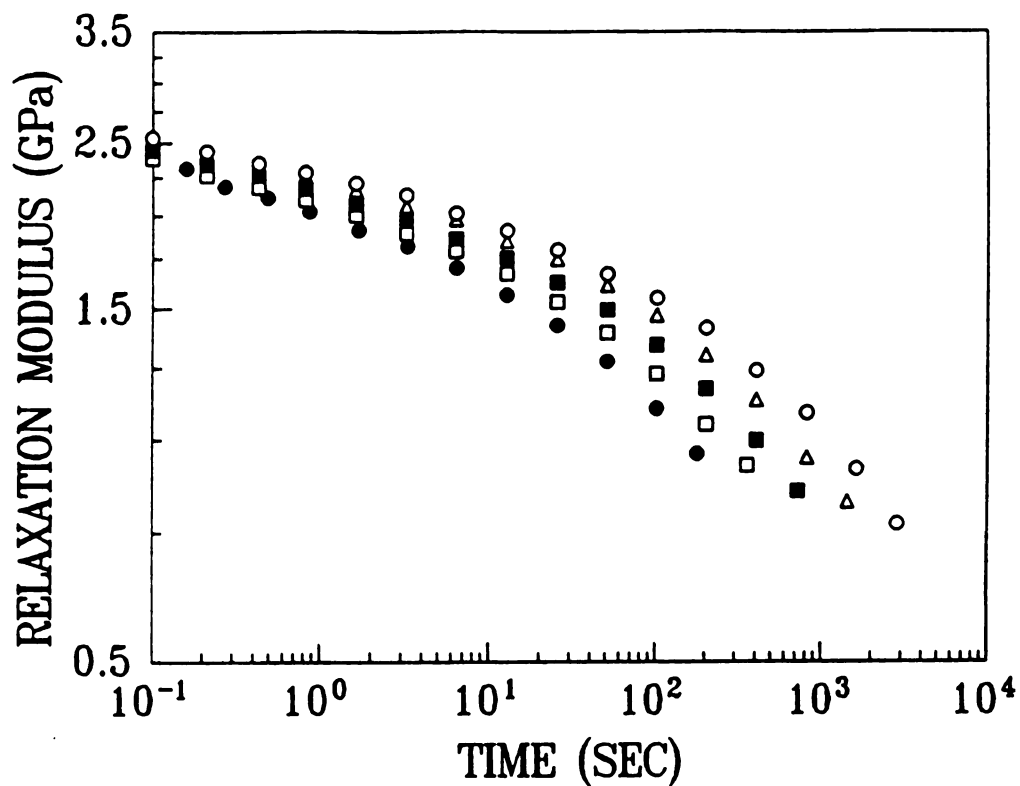


Figure 42. Stress relaxation curves for DGEBA + 95%D230 + 5%D2000 quenched from 102° C (i.e. 20° C above T_g of DGEBA/D230) to 51.2° C and kept at 51.2 ± 0.3° C for a period of time. The applied strain is 0.1%. The different curves were measured at various aging time indicated: (●) 60 min; (□) 120 min; (■) 240 min; (Δ) 480 min; (○) 960 min

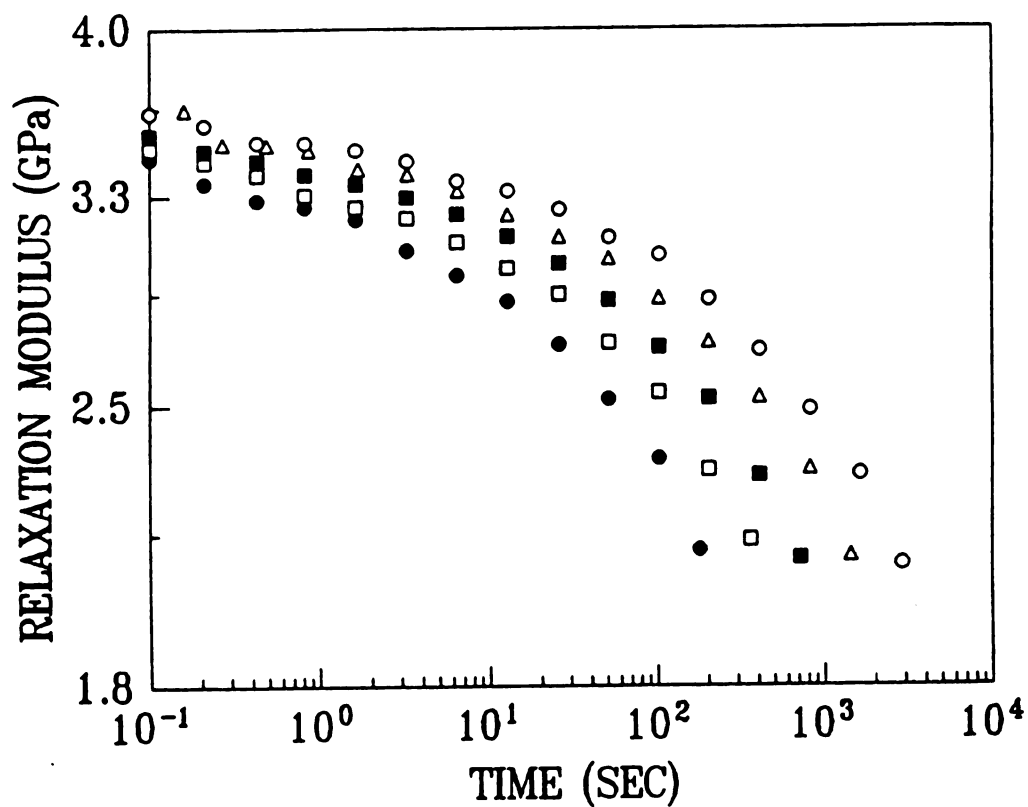


Figure 43. Stress relaxation curves for DGEBA + 90%D230 + 10%D400 quenched from 102° C (i.e. 20° C above T_g of DGEBA/D230) to 51.2° C and kept at $51.2 \pm 0.3^\circ$ C for a period of time. The applied strain is 0.1%. The different curves were measured at various aging time indicated: (●) 60 min; (□) 120 min; (■) 240 min; (Δ) 480 min; (○) 960 min

values of E_0 and β do not vary with aging time for any given epoxy networks, these relaxation curves can be shifted along the time axis to form a single master curve. When increasing the D2000 content, the width of the viscoelastic spectrum decreases and the retardation spectrum also decrease. Although time-aging time superposition appears to be valid for these epoxy networks, the time-crosslink density superposition is not in these stress relaxation tests.

The time-temperature superposition was also investigated. Figure 44 depicts a series of stress relaxation curves at a constant aging time (480 min) as a function of temperature below T_g . The master curve can be obtained by simple horizontal shifting of the curves along the time axis combined with small amount of vertical shifting. The arrow pointed to the shifting direction. The temperature shift factor, a_T , can be obtained from equation 5.

The double-logarithmic plot of aging time shift factor a_t versus t_c for these epoxy networks at $T_g - 15^\circ \text{C}$ present in Figure 45, suggest that as the fraction of D2000 is increased the rate of shifting (the slope of the plot) decreases. As can be seen, there is no significant difference between the responses in these two experiments. This demonstrates that, in spite of the viscoelastic range, the response of the glass aging process has not changed.

Figure 46 show $\log a_T$ versus $T - T_g$ at aging time 480 min for sample of DGEBA+95%D230+5%D2000. The reference was chosen at a temperature approximately 15°C below T_g . There are two regions of behavior. At lower value of $T - T_g$ there is a linear temperature dependence. For $T - T_g = -10$ to -15°C there is a rapid

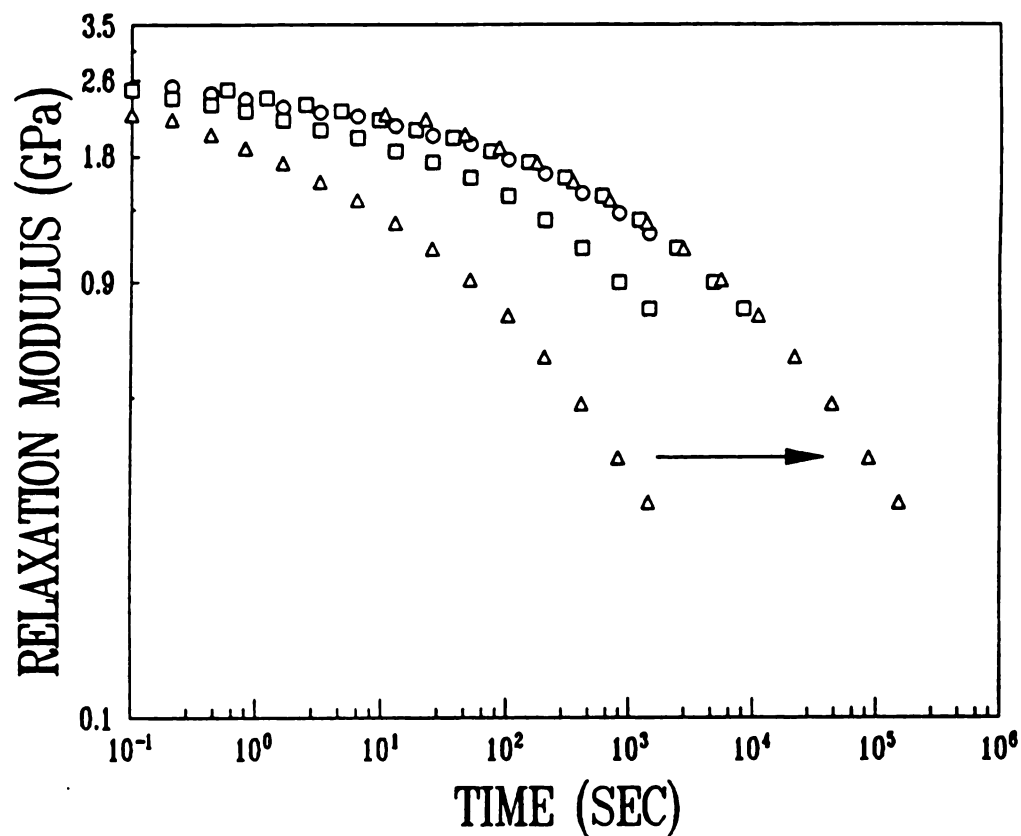


Figure 44. Stress relaxation curves for DGEBA + 95%D230 + 5%D2000 quenched from 102° C to variant temperature for 480 min. The applied strain is 0.2%. The curvatures of these curves were same, the master curves resulting from a superposition by shifting the datas along the axis, so the time-temperature superposition were applied. The temperature (° C): (Δ) 55.2; (□) 51.2; (O) 45.1 (the shifting reference temperature)

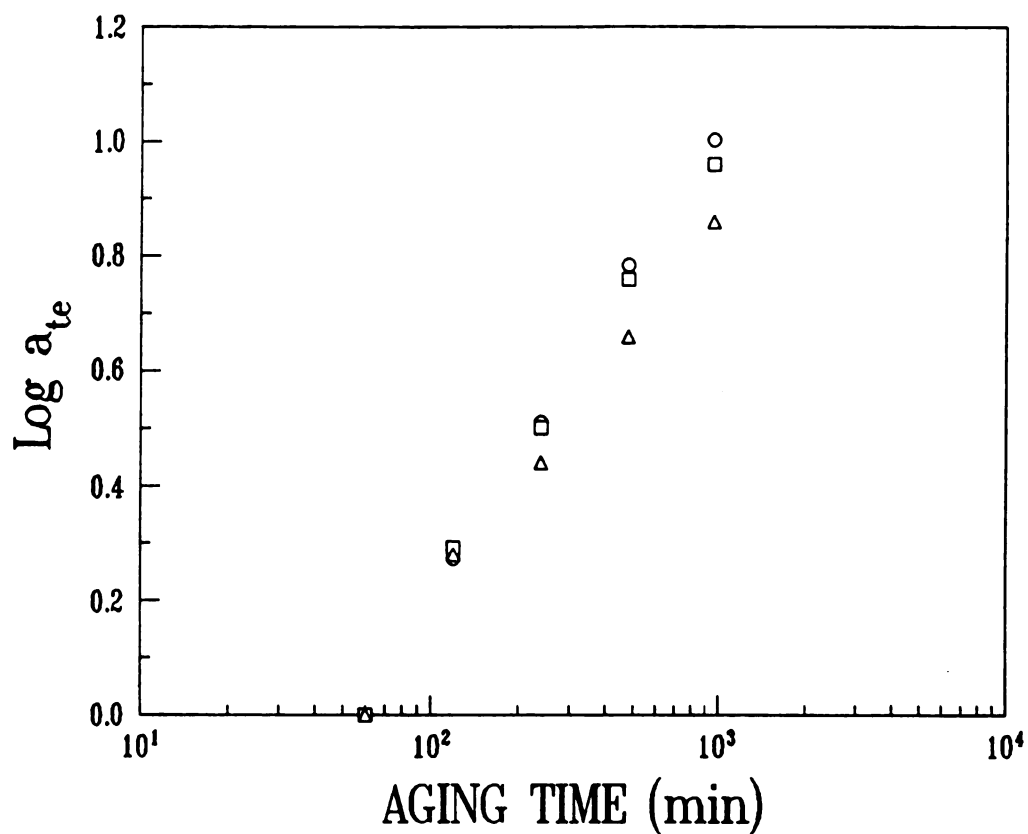


Figure 45. Double logarithmic plot of aging time shift factor a_{te} versus aging time for $T_g - 15^\circ \text{C}$, the reference aging time was chosen as 60 min for each sample. The applied strain is 0.1%. (O) DGEBA + 100%D230; (□) DGEBA + 98%D230 + 2%D2000; (Δ) DGEBA + 95%D230 + 5%D2000

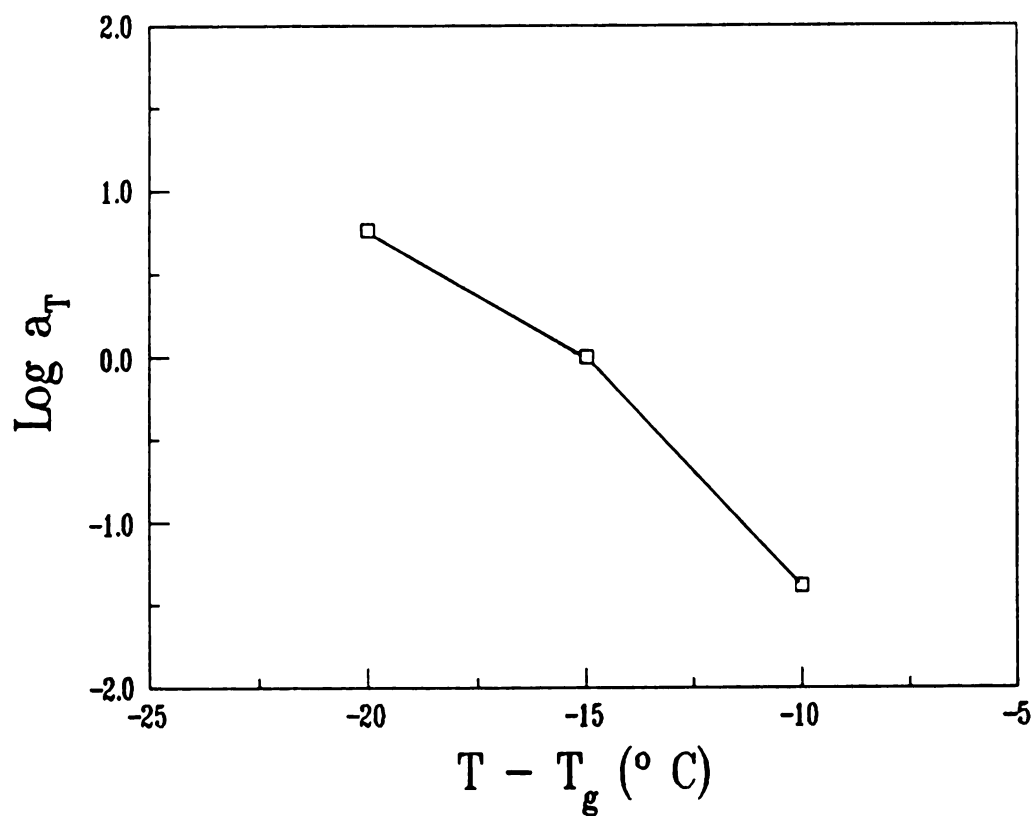


Figure 46. Log of temperature shift factor a_T versus temperature difference $T - T_g$ for DGEBA+95%D230+5%D2000 at aging time 480 min. For $T - T_g = -10$ to -15°C a_T decreases rapidly; this is apparently a transition region from linear dependence to a WLF type dependence on temperature

decrease in shift factor; this is apparently a transition region from the linear dependence to a WLF [31] type dependence on temperature. This result is similar to the results reported by Lee and McKenna [30] of a study on a sample of DGEBA+100%D230.

Table 9. KWW curve fitting parameters for $T_g - 15^\circ \text{C}$; ϵ is 0.1%

Sample	t (min)	E(t) (GPa)	τ (s)	β
DGEBA+100%D230 $T^* : 67.9^\circ \text{C}$	60	3.67	1346.04	0.34
	120	3.68	2056.04	0.34
	240	3.77	4109.01	0.33
	480	3.79	7644.05	0.34
	960	3.80	13599.01	0.34
DGEBA+98%D230+2%D2000 $T^* : 60.8^\circ \text{C}$	60	3.43	347.01	0.23
	120	3.37	683.44	0.24
	240	3.27	1215.41	0.24
	480	3.42	2139.61	0.24
	960	3.56	3382.01	0.23
DGEBA+95%D230+5%D2000 $T^* : 51.2^\circ \text{C}$	60	2.91	118.04	0.21
	120	2.82	227.38	0.21
	240	2.86	329.88	0.21
	480	2.89	545.09	0.21
	960	2.89	857.62	0.21
DGEBA+90%D230+10%D400 $T^* : 61.0^\circ \text{C}$	60	3.52	1652.11	0.32
	120	3.55	3272.31	0.31
	240	3.58	5338.61	0.32
	480	3.66	11641.01	0.29
	960	3.65	20570.01	0.30

T^* : aging temperature for each sample

CHAPTER 4 CONCLUSIONS

The effect of crosslink density distribution on mechanical response of physically aged epoxy glasses were investigated. The Differential Scanning Calorimeter (DSC) results show that the glass transition is broadening with addition of D400 or D2000 content, in particular the glass transition temperature (T_g) decreases with increases of D400 or D2000. But the epoxy networks are still a single phase system, and the value of ΔC_p at T_g increases in this random length network. These results are contradict with previous study by Lee and McKenna [5] that the ΔC_p at T_g no longer changes as function of T_g in the homogeneous length network.

In fracture test, as expected, toughening is achieved for the DGEBA/D230/D2000 networks, it was found that the fracture toughness of this epoxy network increases marketly with increasing D2000 content in this epoxy networks. The fracture toughness also increases with longer aging time for network containing high fraction of longer molecular weight diamine. This result is in contradiction with Struik's [6] understanding the ductile to brittle transition during physical aging. I believe, this is due to the high mobility of D2000 fraction in this network for amorphous polymer. Therefore as the network aged into equilibrium, the D2000 species congregate together, this causes the ductile failure at longer aging time.

In viscoelastic response, the creep compliance curves and stress relaxation curves at different aging time and aging temperature were able to be superimposed and form master curves, thus demonstrating the applicability of the classical time - aging time; time - temperature superposition principle to each these of networks. Although the time - crosslink density superposition is not. Furthermore, it is possible to define a double logarithmic aging rate, μ , which depends on the ratio of the bimodal molecular weight distribution. The double-logarithmic shift rate μ decreases as the D2000 content increase. The aging process is slow down by containing the long chain D2000 which is already in equilibrium state. As increasing the D2000 contents, the viscoelastic spectrum is broadening, this is indicated by the width of the relaxation time β decreases at same temperature range. This phenomenon is observed in both creep and stress relaxation experiments.

REFERENCES

1. Wu, Wenli and Bauer, Barry J., *Macromolecules*, **19**, P1613, 1986.
2. Matsamoto, D. S. *Polym. Eng. Sci.*, **28**, P1313, 1988.
3. Tant, M. R. and Wilkes, G. L. *Polym. Eng. Sci.*, **21**, P874, 1981.
4. Johari, G. P. *J. Chem. Phys.*, **77**, P4619, 1982
5. Lee, A. and McKenna, G. *Polymer*, **29**, P1812, 1988.
6. Struik, L.C.E. '*Physical Aging in Amorphous Polymers and Other Materials.*' Elsevier, Amsterdam, 1978.
7. Ferry, J. D. '*Viscoelastic Properties of Polymers.*' 3rd Edn, Wiley, New York, 1980.
8. Kovacs, A. J., Stratton, R. A. and Ferry, J. D. *J. Phys. Chem.*, **67**, P152, 1963.
9. Struik, L. C. E. *Polymer Eng. and Sci.*, **17**, P165, 1977.
10. Petrie, S. E. B. *Am. Soc. for Metals*, Metal Park, Ohio, 1975.
11. Matsuoka, S. and Bair, H. E. *J. Appl. Phys.*, **48**, P4058, 1977.
12. Baumens-Crowet, C. and Bauwens, J. C. *Polymer*, **23**, P1599, 1982.
13. Bubeck, R. A., Smith, P. B. and Bales, S. E., '*Order in the Amorphous State of Polymers.*' Plenum, New York, 1987.
14. Neki, K. and Geil, P. H., *J. Macromol. Sci., Phys.*, **B8**, 295, 1973.
15. Petrie, S. E. B., *J. Macromol. Sci., Phys.*, **B12**, 225, 1976.
16. Struik, L. C. E. *Ann. N. Y. Acad. Sci.*, **279**, 78, 1976.
17. Petrie, S. E. B. *J. Polym. Sci. Polym. Phys. Ed.*, **10**, P1255, 1972.

18. Ali, M. S. and Sheldon, R. P. *J. Appl. Polym. Sci.*, **14**, P2619, 1979.
19. Young, R. J. and Kinloch, A. J., '*Fracture Behavior of Polymers*, Applied Science Publishers, London, 1983.
20. Kunz, S. C., Sayre, J. A. and R. A. Assink, *Polymer*, **23**, P1897, 1982.
21. Lovell, P. A. and Young, R. J. '*Introduction to Polymers*. 2nd ed. Chapman & Hall, 1991.
22. Bucknall, C. B. and Gilbert, A. H. *Polymer*, **30**, P213, 1989.
23. Williams, J. G. *Fracture Mechanics of Polymers*, Ellis Harwood, Chichester, 1989.
24. P. Musto, G. Ragosta and G. Scarinzi, *J. Polym. Sci., Part B. Polym phys.*, **32**, P409, 1994.
25. Golden, J. H., Hammant, B. L. and Hazel, E. A., *J. Appl. Polym. Sci.*, **11**, 1571, 1967.
26. Lee, A. and McGary, J. *J. Mater. Sci.* **26**, P1, 1991.
27. Brohtman, L. J. and Krishnakumar, S. M. *Polym. Eng. Sci.*, **16**, P74, 1976.
28. Kohlrausch, R. *Pogg. Ann. phys.*, 1847, **12**, 393.
29. Williams, G. and Watts, D.C. *Trans, Faraday Soc.*, **66**, P80, 1970.
30. Lee, A and Mckenna, G. (1990). *Polymer*, **31**, P423, 1990.
31. Willams, M. L., Landel, R. F. and Ferry, J. D. *J. Am. Chem. Soc.*, **77**, P3701, 1955.

MICHIGAN STATE UNIV



312930141